

In situ gasification Chemical-Looping Combustion of coal using limestone as oxygen carrier precursor and sulphur sorbent

A. Abad*, M. de las Obras-Loscertales, F. García-Labiano, L. F. de Diego, P. Gayán, J. Adánez

Department of Energy and Environment. Instituto de Carboquímica (ICB-CSIC).

C/Miguel Luesma Castán 4,50018 Zaragoza.

* Corresponding author: abad@icb.csic.es;

Phone: + 34 976 733 977; Fax: +34 976 733 318

Abstract

In-situ Gasification Chemical-Looping Combustion (iG-CLC) burning coal is achieving a great interest due to the possibility of using low cost oxygen carriers such as CaSO_4 . The Limestone Chemical Looping Combustion process (LCL-CTM) registered by Alstom Power Inc. proposes the use of a continuous CaCO_3 feeding together with coal to produce CaSO_4 as an oxygen carrier via sulphur retention. The operation is similar to what happens in a circulating fluidized bed boiler burning coal. In the present research work, the study of thermodynamic equilibrium limitations together with mass and enthalpy balances have been carried out for a CLC system in order to investigate whether the LCL-CTM process is a promising and energy efficient option to carry out the coal combustion with CO_2 capture and in-situ desulphurisation. So, no limitations were found to transfer the required oxygen from air to fuel using sulphated limestone as oxygen carrier for whatever coal used. However, coals with sulphur content above 1 wt.% are advisable to perform this process. In addition, no drawback referred to thermal integration in the system has been detected. Thus, operation at 950 °C in the fuel reactor

to avoid SO₂ release via side reactions, and 1000 °C in the air reactor is feasible. Likewise, experimental tests have been performed in a thermogravimetric analyser to analyse the capability of a limestone to be sulphated and to transfer oxygen. A value of the oxygen transport capacity of about 16.7 wt.% was obtained. This value is four times higher than that of others typical inexpensive oxygen carriers published in literature.

Keywords: CO₂ capture, Chemical Looping Combustion, Coal, Desulphurization, Calcium-based sorbent, Oxygen carrier.

1 Introduction

Nowadays, it is globally recognized that the release of greenhouse gases, and especially CO₂, into the atmosphere from fossil fuel combustion in power plants is the mainly responsible for the so-called Global Warming. Recently, the 21st United Nations Climate Change Conference (COP21) [1] was celebrated in Paris where representatives of 195 countries were present in order to slow down the increase of atmospheric CO₂ in the future. The main agreement reached was to maintain the increase of global temperature below 2 °C with respect to pre-industrial period, that is, not to reach CO₂ concentration in the atmosphere higher than 450 vppm. Several options are needed to minimize CO₂ emissions in a short-medium term such as reducing energy consumption, using renewable sources, fossil fuel with low carbon content, nuclear energy as well as CO₂ capture and storage (CCS) technologies [2].

In this context, Chemical Looping Combustion (CLC) is a promising technology to carry out the CO₂ capture at low economic and energetic cost. CLC is based on the transfer of the oxygen from air to the fuel by means of a solid oxygen carrier to avoid the direct contact between air and fuel. The majority of the CLC plants use the

configuration composed of two interconnected fluidized bed reactors, fuel and air reactors with a particulate oxygen carrier circulating between them [3].

The CLC technology to burn solid fuels like coal is achieving a high degree of development [3,4] since it is expected that they continue being one of the main energy sources in a medium term [5]. Among the different approaches to perform the combustion of solid fuels in CLC systems, the *in-situ* Gasification CLC (*iG-CLC*) is focusing great attention because of the possibility of using low cost oxygen carriers [6]. In *iG-CLC*, the solid fuel is introduced and mixed with the oxygen carrier in the fuel reactor where it is directly gasified by steam and/or CO₂; see Fig. 1. Then, the coal gasification products are burnt by the oxygen carrier via a gas-solid reaction. Once the oxygen carrier is reduced in the fuel reactor, it is transported to the air reactor to be oxidised in order to start a new redox cycle. The net chemical reaction as well as the heat involved in the global process is the same as for usual combustion.

In *iG-CLC*, the CO₂ capture efficiency greatly depends on the char gasification rate which is the limiting step. To maximize the char conversion in the fuel reactor, thus increasing the CO₂ capture, high reactor temperature and the use of a highly reactive oxygen carrier are advised to increase the char gasification rate [7]. But the use of a highly efficient carbon separation system, e.g. a carbon stripper, is required in order to reach CO₂ capture rates close to 100%; see Fig. 1 [8]. Thus, CO₂ capture efficiency values close to 100% were reached in a 100 kW_{th} CLC unit [9] by using a highly efficient carbon stripper [10].

A critical aspect in deploying the CLC technology is to select an appropriate oxygen carrier. In the case of CLC with solids, the cost of the oxygen carrier and its environmental friendly behaviour are very relevant characteristics since it is inevitable that some oxygen carrier particles are extracted with the coal ashes when they are

removed from the system. Therefore, the use of natural ores or by-products from industrial processes, which are inexpensive and widely available, could be a promising option to develop *iG-CLC* technology. Up to now, most of the studies have been focused on iron-based materials from different origins such as ilmenite, which has been intensively used in pilot units from 0.5 kW_{th} to 1 MW_{th} burning coal [9,11-15]. In these cases, complete combustion was not achieved, and unconverted products such as H₂, CO and CH₄ are present in the CO₂ stream exiting the fuel reactor. Combustion efficiency has been improved by using more reactive materials, e.g. iron and manganese ores or waste Fe-enriched sand fraction from alumina production, but complete combustion was still not reached [16-18]. In addition, several design improvements have been evaluated in order to enhance the combustion efficiency [19].

Besides, the use of materials with the capability to release gaseous oxygen in the fuel reactor have been proposed to improve the *iG-CLC* performance, in the so-called Chemical Looping with Oxygen Uncoupling (CLOU) [20]. Thus, synthetic materials based on copper oxide, have shown excellent performance regarding combustion efficiency [21] whereas the oxygen uncoupling capability of Mn-Fe and Ca-Mn materials improved the combustion efficiency of coal and wood char [18,22].

In addition to these materials, sulphated limestone has been used as oxygen carrier in a 3 MW_{th} CLC unit by Alstom in the so-called Limestone Chemical Looping Combustion process, LCL-CTM [23]. In the LCL-CTM process either CaSO₄ formed *in-situ* by the limestone reaction with sulphur from coal or CaSO₄ present in ash from coal combustion in a circulating fluidized bed (CFB) is proposed as an oxygen carrier material. Nevertheless, with the exception of the fact that a good performance regarding CO₂ capture was achieved [24], there is no detailed information available in literature regarding the LCLTM process. These excellent results would be attributed to the use of a

novel oxygen carrier (sulphated limestone) and/or the conceptual design of the 3 MW_{th} CLC unit. New advances and future perspectives have been recently reported [25].

The main chemical reactions involved in the *i*G-CLC process using CaSO₄ as oxygen carrier are compiled in Table 1. Desired reactions in the fuel reactor are referred to combustion of CO, H₂ and CH₄ (R1-R3).

The advantages in the use of CaSO₄ as an oxygen carrier are its broad availability, low cost and high oxygen transport capacity. The oxygen transport capacity of CaSO₄ is 47 wt.% which is considerably higher than any other metal oxide based material [3]. Nevertheless, this mineral may present some drawbacks such as its low reactivity compared to other materials and the fact that undesired SO₂ can be released at temperatures of interest for CLC due to side reactions R4-R8. These reactions are undesired because SO₂ is emitted together with the combustion products and, most important, the oxygen transport capacity of CaSO₄ is diminished.

Several authors have evaluated the use of anhydrite ore, a mineral which is mainly composed of CaSO₄, for CLC [26-42]; but not sulphated limestone. Song et al. [26] observed that both reduction R1 and side reactions R4 and R7 were enhanced by increasing temperature. It was found that CaS was the dominant compound after CaSO₄ reduction at 900 °C, whereas the presence of CaO was more relevant at 950 °C. Further works have also observed the same effect of the temperature on side reactions [27-30]. Shen et al. [30] reported that the solid-solid reaction R7 was the mainly responsible for CaSO₄ decomposition and proposed 900-950 °C and 1050-1150 °C as a suitable range of temperatures for the fuel and the air reactors, respectively.

Sulphur evolution could be also a problem in the air reactor, where CaS is oxidised to CaSO₄ through reaction R9. In this case, evolution of SO₂ can also occur via undesired reactions R7, R8 and R10.

Several alternatives have been proposed in order to avoid the release of SO₂ from CaSO₄ in both reactors. Some studies have reported that the addition of Fe₂O₃ to CaSO₄ by impregnation method [31] or mechanically [32,33] or physically mixed [34] may contribute to inhibit undesired side reactions. Tian et al. [28,35] observed by thermogravimetric analysis that CaSO₄ presented higher reactivity with H₂ than with CO and that solid reactive products were almost pure CaS when the partial pressure of CO or H₂ was 40 kPa or higher. They proposed to carry out a partial combustion of the fuel in a CLC unit with CaSO₄ and subsequently, the complete combustion of product gases might be performed in another CLC system using nickel oxide as oxygen carrier [28].

Moreover, kinetic studies have been carried out to determine the most relevant reaction mechanism involved in CaSO₄ reduction [36-40]. Xiao et al. [36] determined the kinetics of reduction of CaSO₄ with CO in an isothermal differential bed reactor. They concluded that the dominant reaction CaSO₄ with CO to form CaS and CO₂ was controlled by the shrinking core model with both chemical reaction and product layer diffusion. Zheng et al. [37] investigated the parallel reactions of CaSO₄ with CO using a nucleation and growth model from TGA data obtaining well-fitting results. Similar conclusions were reported by Tian et al. analysing the behaviour of CaSO₄ reduction with CO [38] and in pure nitrogen atmosphere [39] in which the reaction was controlled by a nucleation mechanism.

Other authors have suggested introducing CaO or CaCO₃ together with CaSO₄ [41] to capture the SO₂ released during CaSO₄ decomposition. Further studies revealed that

CaSO₄/CaCO₃ prepared by a mechanical mixing method could also inhibit the aggregation of CaSO₄ oxygen carrier particles during the process at high temperature [42]. This effect could be limited by the sulphation capacity of the sorbent in the CaO/CaSO₄ mixture. This problem could be solved in the LCL-CTM process, where only a continuous CaCO₃ feeding is performed together with coal, similar to the operation in coal combustion in CFB boilers [43].

The objective of this work was to get an insight into the LCL-CTM process, where sulphated limestone in the CLC system is used as an oxygen carrier. The study of thermodynamic equilibrium limitations together with mass and enthalpy balances for the CLC system were carried out to investigate whether the LCL-CTM process is a promising and energy efficient option to carry out the coal combustion with CO₂ capture and *in-situ* desulphurisation. Parameters such as [Ca/S] molar ratio as well as ash and sulphur content of coal were analysed. In addition, experimental redox cycles in a thermogravimetric analyser (TGA) were carried out to analyse the capability of a limestone to be sulphated and to transfer oxygen. Composition and reactivity evolution of the oxygen carrier with the number of redox cycles were studied.

2 Assessment of *i*G-CLC of coal using sulphated limestone as oxygen carrier

2.1 Description of the process

Alstom Power Inc. has registered a patent referred to the CLC process using sulphated limestone (CaSO₄) as an oxygen carrier, LCL-CTM [44]. Fig. 2 illustrates the flow diagram of this process. For the commissioning of the plant, firstly the bed is filled with either anhydrite ore or ashes from coal combustion from CFB combustors. Then, coal and limestone are fed into the fuel reactor (FR) of the CLC unit so that limestone is

calcined to CaO (R11) and coal is gasified by steam. CaO captures the sulphur from coal to form CaS at the fuel reactor reducing conditions (R12). The formed CaS is transported to the air reactor (AR) where the oxygen carrier is generated, i.e. CaSO₄ (R9). Once the steady state conditions are reached, CaSO₄ transfers the oxygen to the fuel being reduced to CaS in the fuel reactor (R1-R3). At the outlet of the fuel reactor, a gas stream mainly composed of CO₂ and H₂O is obtained. H₂O may be easily separated from CO₂ by condensation so as to get a highly concentrated CO₂ stream. The gas product at the exit of the air reactor is oxygen-depleted air.

Moreover, a purge line composed of ashes and Ca-based sorbent (CaO and CaSO₄) is installed in order to avoid solids accumulation in the system. The heat released in the whole process is used to produce steam in a series of heat exchangers located inside the air reactor. Likewise, heat flows can be recovered from the solids of the purge stream and from the outlet gas stream of both fuel and air reactors by means of heat exchangers.

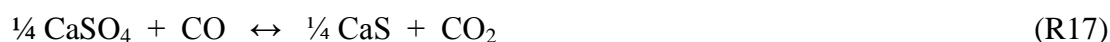
2.2 Thermochemical analysis

Thermodynamic calculation was initially carried out to obtain the equilibrium composition in gas and solid phases using the HSC 6.1 software [45].

2.2.1 Fuel reactor. In the fuel reactor, a solid stream of CaSO₄ and CaO is available to react with the fuel compounds. Combustion of the solid fuel happens mainly using the oxygen present in CaSO₄. But also, sulphur from the fuel is released to gas phase which can react with existing CaO. As a first approximation for thermochemical calculations, a ratio [CaSO₄/CaO]=1 was assumed at the fuel reactor inlet. The oxygen carrier to fuel ratio (ϕ) was fixed to be 9. The parameter ϕ was defined as the oxygen available in the oxygen carrier, i.e. CaSO₄, divided by the oxygen required to burn the fuel. The fuel

was assumed to be solid carbon with sulphur in a ratio $[S/C]=0.1$, which would be characteristic of a coal with a high sulphur content [46]. Also, the steam to carbon ratio was fixed to $[H_2O/C]=1$.

Firstly, a study of the effect of the temperature on the equilibrium composition under atmospheric pressure was performed. Carbon is mostly converted to CO_2 in the entire temperature interval studied, with the corresponding $CaSO_4$ reduction to CaS ; see Fig. 3A. Full combustion is not reached since there is some unburnt CO and H_2 present in the fuel reactor according to the following thermodynamic equilibrium reactions (R17-R18) [45,47]. Nevertheless, the CO and H_2 conversion to CO_2 and H_2O is higher than 99.5 % at temperature of interest in CLC.



$$K_{eq} = \exp\left(0.4579 + \frac{6108}{T} + \frac{293000}{T^2}\right) \quad \text{Eq. (1)}$$



$$K_{eq} = \exp\left(2.875 + \frac{2903}{T} + \frac{767000}{T^2}\right) \quad \text{Eq. (2)}$$

In addition, sulphur from coal is retained by CaO in the form of CaS via reaction R12. Remaining sulphur in gas phase was mainly in the SO_2 form since H_2S can be oxidized by the oxygen carrier; see R13. Then, SO_2 can be captured by remaining CaO (R14). However, $CaSO_3$ is not stable at conditions in the fuel reactor because it can be oxidised to $CaSO_4$ in presence of H_2O or CO_2 ; see reactions R15 and R16.

The effect of the oxygen carrier to fuel ratio on the thermochemical equilibrium was also evaluated; see Fig. 3B. For $\phi > 1$, near complete combustion was achieved, correspondingly to the equilibrium above shown between H_2 - H_2O and CO - CO_2 . At the

chosen temperature (950 °C), there is some SO₂ present in the combustion gases. The avoidance of molecular O₂ in gases justifies this result. Thus, the reverse of reaction R8, which is a common reaction in sulphur retention by Ca-based sorbent in air combustion, cannot happen in the fuel reactor. On the contrary, SO₂ retention must be driven by reaction R14, followed by R15 and/or R16. Therefore, based on the equilibrium diagram, the maximum sulphur retention value that could be reached for full combustion would be near 54%.

Complete combustion was not achieved for $\phi < 1$ because a sub-stoichiometric amount of oxygen was supplied by the oxygen carrier. Thus, some H₂ and CO are present in the combustion products. However, not relevant sulphur compounds, mostly H₂S, are present in the gaseous stream because reaction R12 is governing the sulphur retention whose equilibrium constant is:

$$K_{eq} = \exp\left(-0.0791 + \frac{76330}{T} - \frac{171300}{T^2}\right) \quad \text{Eq. (3)}$$

The presence of unburnt compounds is frequent in the *i*G-CLC system because partial combustion can be found inside the fuel reactor, or even at the fuel reactor exit.[8,19] In this case, a high sulphur retention value close to 100 % may be reached, similar to results showed in Fig. 3B for $\phi < 1$. In this work, both cases corresponding to sulphur retention values of 54 % and 100% have been taken into consideration for the calculation of mass and energy balances.

2.2.2 Air reactor. In the air reactor, CaS is oxidised to CaSO₄ in the presence of air; see reaction R9. In this case, the ratio CaSO₄:CaS:CaO = 1:1:1, as well as an air excess of 10%, was assumed. The absence of CaS in Fig 4b means all of the reduced oxygen carrier is oxidised into CaSO₄ in the air reactor when there is enough oxygen to

regenerate it. SO_2 is present as gas product at temperatures above $950\text{ }^\circ\text{C}$; see Fig. 4 (gas composition). The temperature for the SO_2 release or CaSO_4 decomposition was shifted at higher values than in the fuel reactor due to the presence of oxygen from the air. Depending on the range of the operating temperature ($950\text{--}1150\text{ }^\circ\text{C}$), no more than $10\text{--}250$ vppm of SO_2 from CaSO_4 decomposition is expected. Other minor compound like SO_3 , appears at higher temperatures close to $1050\text{ }^\circ\text{C}$ but this can be considered as negligible.

2.3 Mass and enthalpy balances

An *iG-CLC* plant must be adequately designed to be energy efficient. Therefore it is necessary to obtain an optimal integration between both reactors with the aim of obtaining a safe and proper operation of the CLC unit. This integration depends on several factors such as the type of oxygen carrier and fuel, as well as the solids circulation rate between air and fuel reactors [48]. In this case, the oxygen carrier was CaSO_4 , but other solids compounds must be considered in the solid mixture. CaCO_3 is introduced together with coal as Ca-based sorbent, which generates CaO and CO_2 at the CLC conditions. Also CaS appears as either reduced compound of CaSO_4 or product of desulphurisation in the fuel reactor. Noticeably, ash from coal will be mixed together the oxygen carrier material.

To evaluate the effect of coal composition on the mass and enthalpy balances, three coals were selected to carry out this study, which were used in previous combustion tests by the authors [46,49]. Table 2 shows ultimate and proximate analysis of the coals considered. Chilean coal was selected due to its low sulphur content. Spanish lignites from the Teruel basin and from Alcorisa were chosen not only due to their high sulphur

content but also due to their different ash content. The oxygen demand (Ω_{coal}) needed to obtain full combustion was also included for each coal.

Fig. 2 shows the area used (delimited by dash line) to perform mass and enthalpy balances. Composition of different gas and solids streams, air reactor temperature and heat exchanges in the system was calculated. Table 3 summarizes equations used for the mass balances in both fuel and air reactors.

The following assumptions were adopted:

- The basis for calculation was a coal feeding corresponding to a 1 MW_{th}.
- Limestone, mainly composed of CaCO₃, together with coal was fed to the fuel reactor. The limestone stream was calculated as a function of the [Ca/S] molar used in the process.
- Pre-heated steam (400 °C) was fed to the fuel reactor as fluidising and gasifying gas agent. The steam to carbon ratio was assumed to be [H₂O/C] = 1. This ratio is suitable to carry out the *in-situ* gasification of coal in the fuel reactor [50,51].
- Regarding the thermochemical analysis on sulphur retention discussed in Section 2.2, two situations were considered. A common finding in CLC is combustion efficiency in the range of 90-95% [19]. Then, combustion efficiency was assumed to be 95%. In this case, the sulphur retention was assumed to be complete, SR = 100 %, according to thermodynamic data. In addition, an ideal behaviour with complete coal combustion was analysed. In this case, the efficiency of sulphur retention was 54 %.

- The fuel reactor was considered as adiabatic and its operating temperature was set in 950 °C in order to obtain a char gasification rate relatively high [15] and at the same time a low CaSO₄ decomposition [26,28,52].
- The regeneration of the oxygen carrier was performed in the air reactor by supplying preheated air (400 °C) with an air excess of 10 %. Complete regeneration of CaS to CaSO₄ was achieved.
- All ashes were considered to be extracted from the system through the purge stream from the air reactor. The composition of the purge stream was assumed to be equal to the solids composition in the air reactor.
- Heat from solids was assumed to be extracted from the air reactor, Q_{ext} , and from the solids purge stream, Q_1 . This heat is used to produce steam, and it was necessary to maintain the CLC unit under autothermal conditions [48].

The composition of the solids streams entering and going out of both reactors were calculated by mass balances. These solids streams, which were used as input data to work out enthalpy balances, depended on the coal composition, the [Ca/S] and [H₂O/C] molar ratios, the oxygen carrier to fuel ratio (ϕ) as well as on the sulphur retention (SR) and fuel combustion efficiency (η_{comb}).

The amount of CaCO₃ fed into the fuel reactor was calculated as a function of the [Ca/S] molar ratio and the sulphur content of the coal. CaSO₄ recirculated between the fuel and the air reactors was dependent of the oxygen carrier to fuel ratio (ϕ) and the oxygen demand needed to obtain full combustion (Ω_{coal}). The ashes recirculated from fuel to air reactor were calculated assuming that there is not preferential separation between ashes and sorbent and the CaO recirculated was worked out as a function of the [Ca/S] molar ratio, sulphur retention (SR) and the moles of CaSO₄. No presence of CaS

at the entrance of the fuel reactor was taken into account since complete oxidation of CaS to CaSO₄ in the air reactor was assumed.

Considering the sulphur retention, it was assumed that sulphur coming from the coal reacted with calcined limestone (CaO) to form CaS (R12). In terms of a conceptual overview, in the sulphur retention reaction via CaO, 1 mole of CaO transfers 1 mole of atomic oxygen (see R19) and thus a fraction of CaSO₄ oxygen carrier will not be needed to burn coal. For every 4 moles of CaS which are formed via R19, 4 oxygen atoms are transferred to fuel, thus 1 mole of CaSO₄ is not required to react. In a similar way, because sulphur is captured by the sorbent, the conceptual reaction R20 will not take place and thus a fraction of CaSO₄ in the oxygen carrier will not be necessary to burn the fuel. For every 2 moles of sulphur reacting with CaO, 1 mole of CaSO₄ will not react with the fuel.



These concepts were used to calculate $n_{\text{CaS},\text{red}}$ and $n_{\text{CaSO}_4,\text{outFR}}$ in Table 3. To clarify this concept, Fig. 5 illustrates two examples about the fate of CaSO₄ and CaS in the fuel reactor. Case I: no limestone addition, SR=0 %, [Ca/S] molar ratio=0 and $\phi=1$. Case II: with limestone addition, SR=100%, [Ca/S]=1 and $\phi=1$. It can be seen that when SR=0 %, all CaSO₄ is reduced to CaS according to $\phi=1$ and the sulphur is burnt to SO₂. But when SR=100 %, a fraction of existing CaSO₄ will remain as CaSO₄ after coal combustion because the sulphur is retained by CaO in the form of CaS.

Regarding the air reactor, all the solids leaving the fuel reactor were the same as the solids entering into the air reactor. All the CaS, both recirculated and from sulphur retention process, was oxidized to CaSO₄. Likewise, it was assumed that the

composition of solids in the purge stream was the same as the outlet solids stream of the air reactor.

Enthalpy balances in the fuel and air reactors were also carried out taking into consideration the enthalpy of both gas and solids compounds entering and leaving each reactor. Those balances can be expressed in general terms as:

$$H_{\text{reac}} = H_{\text{prod}} + Q_{\text{ext}} \quad \text{Eq. (4)}$$

Reactants' and products' enthalpy can be worked out as:

$$H_{\text{reac}} = \sum F_{\text{reac},i} h_{\text{reac},i} \quad \text{Eq. (5)}$$

$$H_{\text{prod}} = \sum F_{\text{prod},i} h_{\text{prod},i} \quad \text{Eq. (6)}$$

where the enthalpy of each compound, i , is defined as:

$$h_i = h_i^o + \int_{T_o}^T C_{p,i}(T) dT \quad \text{Eq. (7)}$$

2.4 Mass and enthalpy balances for SR = 100 %

As it was aforementioned, mass and enthalpy balances were calculated assuming that all the sulphur from the coal was captured by the limestone. These cases were selected because it is likely that small amounts of CO and H₂ remain unburnt in *i*G-CLC systems, which corresponds to favourable thermochemical conditions to achieve complete sulphur retention, as it was also discussed in Section 2.2.

Fig. 6 shows the composition of the recirculation stream as well as its oxygen transport capacity as a function of the [Ca/S] molar ratio for the 3 coals.

For a given coal, an increase in the [Ca/S] molar ratio produced a decrease in the percentage of CaSO₄, ash and oxygen transport capacity because they were diluted in

CaO. Then, opposite trend was found for the percentage of CaO since an increase in the [Ca/S] molar ratio involved an increase in the CaO which stay without reacting with the sulphur from coal. Besides, the higher the sulphur content of the coal, the lower the amount of ash in the recirculated stream. Therefore, the use of Teruel or Alcorisa coals, with high sulphur content, presented similar solids composition in the recirculated stream. However, the combustion of Chilean coal, with low sulphur content, exhibited such high ash content in the recirculated stream that the percentage of the other compounds was very low because of dilution.

A theoretical oxygen transport capacity of the sorbent was calculated as a function of the fraction of CaSO₄ present in the solids recirculated.

$$R_{OC} = x_{CaSO_4} R_{o,CaSO_4} \quad \text{Eq. (8)}$$

The oxygen transport capacity (R_o) of CaSO₄/CaS is 0.47 according to the expression:

$$R_{o,CaSO_4} = \frac{m_{ox} - m_{red}}{m_{ox}} \quad \text{Eq. (9)}$$

It is worth mentioning that for typical [Ca/S] molar ratios used in CFB combustors ([Ca/S]=2-3), a high oxygen transport capacity may be obtained using coals with high sulphur content such as Teruel or Alcorisa; see Fig.6.

Once the R_{OC} is known, the solids circulation rate can be calculated as a function of the ϕ parameter; see Fig.7. Calculations showed that composition of the recirculated stream from the air reactor was independent of the oxygen carrier to fuel ratio (ϕ).

According to the hydrodynamic properties of fluidized bed boilers, a maximum value of 80 kg m⁻² s⁻¹ can be considered for the solids circulation flow in CLC systems [48]. In addition, an optimum value of 0.25 m²/MW_{th} for the cross section area was calculated

considering both the gas velocity and pressure drops required in air and fuel reactors [51]. Thus, a maximum circulation rate would correspond to 20 kg/s per MW_{th} . Taking into account this value, from Fig. 7, it can be concluded that the LCL-CTM process could operate in a broad interval of ϕ values regardless the coal used.

Without becoming problematic, the required solids circulation rate to burn the Chilean coal is higher than in the other cases, which is related to the more diluted $CaSO_4$ in the stream of solids. So, no limitations could be found to transfer the required oxygen from air to fuel in the *i*G-CLC system using sulphated limestone as oxygen carrier for whatever coal used.

Fig. 8 depicts the effect of oxygen carrier to fuel ratio and [Ca/S] molar ratio on the air reactor temperature ($T_{FR} = 950^\circ C$). It was observed that the temperature in the air reactor was almost the same regardless of the [Ca/S] molar ratio used and for a given oxygen carrier to fuel ratio. Furthermore, temperatures below 1000 °C were obtained in all the cases in which the criterion of the maximum solids recirculation (20 kg/s per MW_{th}) was considered. Therefore, the use of sulphated limestone as oxygen carrier could be a promising alternative which would allow operating at temperatures close to 950 °C in the fuel reactor and below 1000 °C in the air reactor. Likewise, a feasible integration between both reactors could be achieved at desired conditions in order to minimize sulphur evolution in exhaust gases both the fuel and air reactors.

Fig. 9 illustrates the influence of the oxygen carrier to fuel ratio (ϕ) on the heat extracted from the air reactor for different [Ca/S] molar ratios fed into the fuel reactor. Apparently, a different behaviour is found for Teruel and Alcorisa in comparison with the Chilean coal, which is mainly attributed to the different sulphur content. For Alcorisa and Teruel coals, an increase in the [Ca/S] molar ratio fed into the fuel reactor

causes a relevant decrease in the heat extracted from the air reactor. This is due to the close balance between heat extracted in the air reactor and enthalpy contained in the purge stream of solids. Thus, a rise in the [Ca/S] molar ratio involves an increase in the limestone feeding. As a consequence, a higher amount of hot solids has to be removed from the system through the line purge which leads to a heat loss in the air reactor. This means that less heat is needed to be removed from the air reactor, i.e. Q_{ext} decreases as [Ca/S] increases. However, the [Ca/S] molar ratio hardly affects the heat released in the air reactor for the Chilean coal because of its low sulphur content. So, the amount of sorbent supplied to the combustor is so small that it hardly affects both the flow of solids in the purge stream and the heat removed from the air reactor. For the same reason, the heat removed from the air reactor increases as the ash content in coal decreases. Moreover, the heat extracted from the system decreases as the oxygen carrier to fuel ratio diminishes. This is typical in CLC systems because it is associated with the fact that the air reactor temperature increases as the oxygen carrier to fuel ratio decreases.[48] Therefore, the enthalpy of the outlet gas stream from the air reactor increases and as a consequence of that, a lower amount of heat must be extracted from the air reactor.

2.5 Mass and enthalpy balances for SR < 100%

Furthermore, the calculation of energy balance assuming full coal combustion which corresponds to sulphur retention of 54% was performed. The effect of oxygen carrier to fuel ratio and [Ca/S] molar ratio on the heat extracted from the air reactor, temperature in the air reactor and solids recirculation rate was analysed using Teruel lignite as fuel. Fig. 10 shows the results obtained comparing both cases, i.e. SR=100 % and SR=54 %. Similar trend with ϕ to those observed when there were some unconverted CO and H₂ was found; see Figs. 7-9. As it was expected, lower sulphur retention value causes an

increase in the solids circulation rate due to less CaSO_4 is formed. As a consequence, the temperature in the air reactor is slightly lower than that for sulphur retention values of 100 %, and therefore, the heat extracted from the air reactor is slightly higher when $\text{SR}=54$ %.

2.6 Effect of coal composition (S and ash)

With the aim to select what type of coal would be more appropriate for the *iG-CLC* process using calcium-based sorbents as oxygen carrier, a general study of the effect of ash and sulphur content of coal on the main operating variables (heat extracted from air reactor, air reactor temperature, solids circulation rate and oxygen transport capacity) was performed.

For this purpose, several coal compositions were simulated, keeping constant the C:H:O:N:H₂O ratio in coal. The range of sulphur and ash content varied from 0.2 to 7 wt.% and from 5 to 30 wt.%, respectively. For all the cases, a [Ca/S] molar ratio of 3 and oxygen carrier to fuel ratio of 10 were chosen in order to achieve suitable temperatures in the air reactor, that is, below 1050 °C.

Fig. 11 shows the effect of ash and sulphur content of coal on the main variables in 3D representation. The solids circulation rate decreased by decreasing the ash and/or by increasing the sulphur content; see Fig. 11A. In both cases, the amount of oxygen carrier is more concentrated in the solids stream as the ash content is lower and/or the amount of CaSO_4 formed, i.e. the oxygen carrier, is higher. The increase of the solids circulation rate is especially relevant for coals with sulphur content lower than 1 wt.%.

More sulphur and/or less ash in coal favour the increase of the oxygen transport capacity of the circulating solids. Note that the trend of the solids circulation rate was closely linked to the variation of the oxygen transport capacity with sulphur and ash

content; see Fig. 11A and 11B. Thus, the oxygen transport capacity increased by increasing the sulphur and by decreasing the ash content of the coal, thus decreasing the required flow of recirculated solids.

In the same way, the temperature in air reactor also increased by decreasing the ash and by increasing the sulphur content of the coal; see Fig. 11C. This is because a decrease in the solids circulation rate is associated with a higher difference of temperature between fuel and air reactor [48]. Finally, with regard to heat extracted from air reactor, two opposite effects were detected. On the one hand, an increase in the sulphur content of the coal involved a decrease in the heat flow extracted from the air reactor. This fact was related to the increase of the air reactor temperature. Thus, the gas flow leaving the reactor was hotter and a lower heat flow from air reactor could be extracted. On the other hand, an increase in the ash content of the coal produced a decrease in the air reactor temperature. According to the previous reasoning, this should mean an increase in the heat flow extracted from the air reactor, but the opposite trend to expected was observed, decreasing by increasing ash content; see Fig. 11D. This fact was related to the heat flow taken out of the solids purge which increased with the ash content and was more relevant than the effect of the temperature variation of gases exiting the air reactor. Therefore, the heat flow needed to be extracted from air reactor was lower.

Based on these results, it would be necessary to reach a compromise among the different variables to find the most adequate type of coal for *iG-CLC* systems. To fulfil the maximum circulation rate corresponding to 20 kg/s per MW_{th} with an oxygen carrier to fuel ratio of 10, the use of coals with relatively high sulphur content, above 1 wt.%, could be suitable for the entire range of ash content analysed. For coals with lower sulphur content, the oxygen carrier to fuel ratio should be below 10. For example, for

Chilean coal, the suitable oxygen carrier to fuel ratio would be below 5, see Fig. 7 and 8.

In summary, it is remarkable the high oxygen transport capacity of solids compared to other materials frequently used as oxygen carrier, e.g. ilmenite ($R_{OC}=4$ wt.%) [53] or Fe-ore ($R_{OC}=2.4$ wt.%) [54]. Thus, the required solids circulation rate is lower in LCL-CTM than in *i*G-CLC with ilmenite or Fe-ore and, correspondingly, the mean residence time of solids in the fuel reactor would increase. This fact would increase greatly the char conversion, and therefore the CO₂ capture [7,15]. Nevertheless, high temperature would promote the release of sulphur from the fuel and/or air reactor. So, the temperature in the fuel reactor for sulphated limestone would be lower than for ilmenite or Fe-ore which was suggested to be around 1000 °C [15,55]. In order to avoid a high SO₂ released from side reactions temperature in the fuel reactor would be below 950 °C [26]. This aspect leads to a decrease in the char gasification rate. Regarding this limitation of temperature, it would be necessary to evaluate the effect of the existence of a relevant amount of CaO in the solids streams. Thus, it is well known that this CaO could retain the sulphur released by side reactions [56]. In this case, the limitation of the reactor temperature would be overcome.

3 On the capability of limestone to become an oxygen carrier

As described in Section 2.1., limestone (CaCO₃) is the calcium source to form the oxygen carrier in the form of CaSO₄. To evaluate the capability of a limestone to form CaSO₄, and then to be cyclically reduced by a fuel gas and oxidized by air, some tests were carried out in a TGA.

3.1 Experimental

Granicarb limestone (100-300 μm) which is mainly composed of CaCO_3 , was selected as raw material to study the behaviour of sulphated sorbents as an oxygen carrier. Table 4 shows the chemical composition of the limestone used.

The capability of limestone as sorbent for sulphur retention and oxygen carrier was evaluated with the number of redox cycles by means of experimental tests performed in a TGA. In addition, both the evolution of the composition of limestone to become an oxygen carrier and the reactivity of sulphated limestone were analysed.

The reactor coupled to the thermogravimetric apparatus consists of a quartz tube (15 mm ID) vertically placed in an oven that can be operated at temperatures up to 1000 $^\circ\text{C}$. The sample holder was a wire mesh platinum basket (8 mm diameter, 2 mm height). The reacting gas mixture was controlled by specific electronic mass flow controllers and it was introduced at the bottom of the reaction tube. In addition, N_2 flowed through the microbalance head to keep the electronic parts free of corrosive reactant gas. The temperature and the sample mass were continuously recorded in a computer. The detailed description of the TGA can be found elsewhere [57].

The sample was subjected to alternating reducing and oxidizing conditions. For each run, around 80 mg of limestone particles were introduced into the platinum basket. The experiments were conducted at 950 $^\circ\text{C}$ using a total gas flow of 25 $\text{L}_\text{N}/\text{h}$. Heating was performed in air, thus quick calcination happened at the reacting temperature [58], being the mass of the sample (mainly in the form of CaO) of 45 mg approximately. Then, several redox cycles were performed. Each redox cycle consisted of two consecutive steps: (1) Reducing step. A reducing gas composed by 5 vol.% H_2 , and 3000 vppm H_2S (N_2 to balance) was used for 15 min; and (2) Oxidation step. An oxidizing gas composed by 10 vol.% O_2 (N_2 to balance) was used for 10 min. To avoid mixing of fuel

gas and oxygen, nitrogen was introduced for 1 min after each reducing and oxidizing step.

3.2 Results from TGA experiments

Initially, the sample is mainly composed of CaO due to CaCO₃ calcination. Therefore, to start the redox cycles, it is necessary to carry out a previous preparation step of the oxygen carrier. As can be seen in Fig. 12, firstly, the sample, CaO, was subjected to a pre-sulphidation step with the mix of reducing gases, H₂ and H₂S, to form CaS (R12). As a result, an increase in the mass of the sample was registered [59]. Once CaS was formed, redox cycles started with the oxidation period (R9). The sample was oxidized from CaS to CaSO₄ which involved an increase in the sample mass. Subsequently, a reducing period was performed. Two stages well-distinguished were observed during the reduction due to the existence of a competition between the sulphidation (R12) and reduction reactions (R2). In the former stage or first minutes, the reduction reaction predominated over the sulphidation reaction which was associated with a decrease in the mass of the sample. However, the sulphidation reaction was the predominant reaction in the latter stage or last minutes which led to an increase in the mass of the sample. At this stage, the initial CaSO₄ was assumed to be completely reduced to CaS, or decomposed to CaO, as it is below discussed.

Fig. 13 shows the consecutives reduction and oxidation cycles of the Granicarb limestone performed in a TGA for 24 hours. The mass of the oxidized sample was increasing with the number of cycles up to reaching a stable value. Therefore, it could be considered that a stable condition was reached after around 8 hours.

To follow the conversion of CaO to CaS and/or CaSO₄, the composition of solids after reduction and oxidation were calculated after every reduction, sulphidation and

oxidation stage. Complete reduction of CaSO_4 to CaS was assumed after reduction step. Also, CaS and CaO would be present after sulphidation stage. Thus, only CaO and CaS would be present after these steps, and their composition can be easily calculated by knowing the mass of the sample (Eqs. (10)-(11)).

$$n_{\text{Ca},total} = n_{\text{CaO}} + n_{\text{CaS}} \quad \text{Eq. (10)}$$

$$m_{\text{sample}} = 0.056 n_{\text{CaO}} + 0.072 n_{\text{CaS}} \quad \text{Eq. (11)}$$

However, complete oxidation of CaS to CaSO_4 is not likely to be achieved during the oxidation period due to diffusional restrictions [60]. This implies that the sample was composed of three compounds, CaO , CaS and CaSO_4 , which makes impossible the determination of the exact composition of the oxidized limestone sample by only knowing the sample mass.

The CaSO_4 content in the oxidized sample was obtained by complete reduction in 15 vol. % H_2 (N_2 to balance) at 850 °C in the TGA. Reduction conditions were selected in order to avoid the sulphur release to gas phase during the reduction step. Thus, a preliminary study on the sulphur release with reacting temperature was performed by using anhydrite (see Appendix). In order to calculate the evolution of the CaSO_4 content in the oxidised sample with the cycle number, several cyclic experiments were performed with a sequential increase in the redox cycles. In each experiment, the final step consisted of the corresponding step of oxidation at the n cycle, which was followed by a reduction in H_2 at 850 °C, as it was described above.

Once the composition of each period of reduction, sulphidation and oxidation was known, that is, moles of CaO , CaS and CaSO_4 , a study of the evolution of the sulphur

present in the sample was carried out ([S/Ca] molar ratio) assuming that first cycle was covered as shown Fig. 12.

In Fig. 14, the evolution with the cycle number of the molar fraction of Ca as CaSO_4 , x_{CaSO_4} , after every oxidation stage, as well as the variation of the [S/Ca] molar ratio obtained after every oxidation, reduction or sulphidation stage are represented. On the one hand, the fraction of CaSO_4 in the oxidized samples increases with increasing the number of redox cycles since during the reduction step, the sample is capturing sulphur from the H_2S fed together with H_2 in the reducing gas. On the other hand, it was observed that the [S/Ca] molar ratio increases from the oxidation to reduction reaction and from the reduction to the sulphidation reaction since the presence of H_2S in the reduction step balances the influence of side reactions. However, an important decrease in the [S/Ca] was detected from sulphidation to oxidation reaction which may be attributed to the release of SO_2 because of side reactions (R7, R8, R10).

With the calculated mass fraction of CaSO_4 in the oxidized samples, the theoretical oxygen transport capacity, $R_{OC,th}$, is determined as:

$$R_{OC,th} = x_{\text{CaSO}_4} R_{o,\text{CaSO}_4} \quad \text{Eq. (12)}$$

the oxygen transport capacity of CaSO_4 being $R_{o,\text{CaSO}_4} = 0.47$.

In addition, an effective oxygen transport capacity, $R_{OC,eff}$, is defined considering that some sulphur is released to gas phase as SO_2 , which decrease transferable oxygen. As an example, oxygen can be transferred by the R2 and R4.

Obviously, the oxygen transferred via reaction R4 is $\frac{1}{4}$ of the oxygen transferred by R2. The effective oxygen transport capacity was calculated according to the following equation:

$$R_{OC,eff} = \frac{O_{transfer} M_O}{m_{ox}} \quad \text{Eq. (13)}$$

The transferred oxygen in the cycle n is calculated as:

$$O_{transfer,n} = 4n_{CaSO_4,ox_{n-1}} + n_{CaO,ox_{n-1}} - n_{CaO,red_n} - 2d \quad \text{Eq. (14)}$$

the parameter “ d ” being the SO_2 released during the reduction, which is calculated as:

$$d_n = n_{CaSO_4,ox_{n-1}} + n_{CaS,ox_{n-1}} - n_{CaS,red_n} \quad \text{Eq. (15)}$$

n_{CaO,red_n} and n_{CaS,red_n} are the total moles of CaO and CaS generated after the reduction stage without taking into consideration the contribution of the sulphidation reaction with H_2S , respectively. Thus, TGA curves were used to estimate the fraction of $CaSO_4$ being either reduced to CaS or decomposed to CaO (see Annex A).

Fig. 15 shows the evolution of the oxygen transport capacity with increasing the number of redox cycles. As it was expected the oxygen transport capacity rose quickly during the first 5 cycles, and then this increase was of lower relevance for long periods of time. A stable value of the effective oxygen transport capacity of $R_{OC,eff} = 16.7$ wt.% was obtained with this material.

The evolution of the oxygen transport capacity with redox cycles is closely related to the variation of the $CaSO_4$ fraction, as sulphur was increased during the first 5 cycles, and then was slowly increased. Moreover, the theoretical oxygen transport capacity was higher than the experimental one, due to the existence of side reactions which involved a sulphur loss capable of transferring oxygen.

In summarize, from TGA data, a fraction of $CaSO_4$ of 0.23 corresponding to an oxygen transport capacity of 16.7 wt.% would be obtained. In addition, the [S/Ca] ratio in the sample was stabilized in a value around 0.5, which implies that [Ca/S] molar ratio ≥ 2

would be feasible in LCL-CTM process with this limestone for SR = 100%. These values would be suitable with respect to air reactor temperature and solids circulation rate for *i*G-CLC process according to the results previously obtained by mass and enthalpy balances.

In the case of operating at Ca/S molar ratios below 2, the sulphur retention values would be lower than 100% which would be calculated using Eq. (16).

$$SR(\%) = 100 \cdot \left[\frac{S}{Ca} \right]_{sulph} \left[\frac{Ca}{S} \right] \quad \text{Eq. (16)}$$

$\left[\frac{S}{Ca} \right]_{sulph}$ being the sulphur/calcium molar ratio reached just after the sulphidation reaction, see Fig. 14.

A decrease in the sulphur retention value will have a great influence on the solids circulation rate, as it is shown in Fig. 16 for the three coals analysed. From the previous results for SR= 100%, an oxygen carrier to fuel ratio of 2 for Chilean coal and an oxygen carrier to fuel ratio of 10 for both Teruel and Alcorisa coals were selected in order to fulfil the hydrodynamic and temperature limitations established. As can be seen, the influence of the sulphur retention on the solids circulation is more relevant than the Ca/S molar ratio used in all cases.

Using Granicarb limestone, for Ca/S molar ratios above 2 there is no problem in terms of solids circulation for any coal, even for sulphur retention values as lower as 40%. For Ca/S molar ratios below 2, the sulphur retention values decrease and thus higher solids circulation rates are needed (see red line in Fig.16 corresponding to Granicarb limestone).

Nevertheless, because reactivity of the limestone may be different and the R_{oc} strongly depends on it, it would be necessary to carry out further studies with other calcium based sorbents such as limestones and/or dolomites and to evaluate the process at lab-scale plant in order to get an insight into the SO_2 release during the alternating reducing and oxidizing conditions.

4 Conclusions

A comprehensive study on the viability of *i*G-CLC burning coal using sulphated limestone as an oxygen carrier has been carried out by means of mass and energy balances. Thermochemical analysis shows that it is possible to retain sulphur from coal in the fuel reactor to form CaS, which will be oxidized to $CaSO_4$ in the air reactor. A suitable operating temperature in the fuel reactor is 950 °C in order to avoid as much as possible the promotion of side reactions with sulphur release. In addition, the presence of some unburnt compounds favoured the sulphur retention by limestone. Mass balances showed that a solid with high $CaSO_4$ content can be circulated from air to fuel reactors. So, these solids have high enough oxygen transport capacity to transfer oxygen from air to fuel. The process is efficient from an energy point of view. The difference of temperature between both reactors, air and fuel, can be below 50 °C if the requirement of solids circulation rate is fulfilled. Hence, no drawback referred to the integration of both reactors was found. The selection of a suitable oxygen carrier to fuel ratio mainly depends on the sulphur content of the coal used.

Furthermore, preliminary tests have been conducted in a TGA in order to analyse the behaviour of sulphated limestone and to determine its oxygen transport capacity. CaS was formed during reduction in the presence of H_2 and H_2S . Then, CaS was oxidised to $CaSO_4$ in air. Some sulphur release was observed during reduction and oxidation stages, but sulphur increased in the sample during consecutives redox cycles, thus increasing

the oxygen transport capacity up to a value about 16.7 wt.%. This value is four times higher than that of ilmenite which is another inexpensive oxygen carrier used for *iG-CLC* systems.

Results presented in this work shows the technical viability of the *iG-CLC* process using sulphated limestone as oxygen carrier, which was generated *in situ* following the Limestone based Chemical Looping Combustion (LCL-CTM) process by Alstom.

Acknowledgements

The work presented in this article is partially funded by the Spanish Ministry of Economy and Competitiveness (ENE 2014-56857-R, ENE2013-45454-R) and by the European Regional Development Fund (ERDF). A. Abad thanks CSIC for the financial support given to the project 201480E101.

References

- [1] COP21 <http://www.cop21paris.org/about/cop21/>, 2016 (27.03.16).
- [2] IPCC special report on carbon dioxide capture and storage. In: Metz B, Davidson O, de Coninck HC, Loos M, Meyer LA, editors. Cambridge, United Kingdom, New York, NY, USA: Cambridge University Press; 2005. p. 442.
- [3] J. Adánez, A. Abad, F. García-Labiano, P. Gayán and L. F. de Diego, Progress in Chemical-Looping Combustion and Reforming technologies, Prog. Energy Combust. Sci. 38 (2012) 215-282.
- [4] A. Lyngfelt, Chemical-looping combustion of solid fuels – Status of development, Appl. Energy 113 (2014) 1869-1873
- [5] IEA (2013a) International Energy Agency, World Energy Outlook (WEO).
- [6] J. Adánez, P. Gayán, I. Adánez-Rubio, A. Cuadrat, T. Mendiara, A. Abad, F. García-Labiano, L. F. de Diego, Use of Chemical-Looping processes for coal combustion with CO₂ capture, International Conference on Greenhouse Gas Control Technologies, Kyoto, Japan, November, 2011.
- [7] F. Garcia-Labiano, L. F. de Diego, P. Gayan, A. Abad and J. Adanez, Fuel reactor modelling in chemical-looping combustion of coal: 2—simulation and optimization, Chem. Eng. Sci. 87 (2013) 173-182.
- [8] A. Abad, P. Gayán, L. F. de Diego, F. García-Labiano and J. Adánez, Fuel reactor modelling in chemical-looping combustion of coal: 1. model formulation, Chem. Eng. Sci. 87 (2013) 277-293

- [9] P. Markstöm, C. Linderholm and A. Lyngfelt, Chemical-looping combustion of solid fuels – Design and operation of a 100 kW unit with bituminous coal, *Int. J. Greenh. Gas Control* 15 (2013) 150-162.
- [10] A. Abad, J. Adánez, L. F. de Diego, P. Gayán, F. García-Labiano and A. Lyngfelt, Fuel reactor model validation: Assessment of the key parameters affecting the chemical-looping combustion of coal, *Int. J. Greenh. Gas Control* 19 (2013) 541-551.
- [11] N. Berguerand and A. Lyngfelt, Design and operation of a 10 kWth chemical-looping combustor for solid fuels – Testing with South African coal, *Fuel* 12 (2008) 2713-2726.
- [12] A. Cuadrat, A. Abad, F. García-Labiano, P. Gayán, L. F. de Diego and J. Adánez, The use of ilmenite as oxygen-carrier in a 500 Wth Chemical-Looping Coal Combustion unit, *Int. J. Greenh. Gas Control* 5 (2011) 1630-1642.
- [13] A. Thon, M. Kramp, E. U. Hartge, S. Heinrich and J. Werther, Operational experience with a system of coupled fluidized beds for chemical looping combustion of solid fuels using ilmenite as oxygen carrier, *Appl. Energy* 118 (2014) 309-317.
- [14] J. Ströhle, M. Orth and B. Epple, Chemical looping combustion of hard coal in a 1 MWth pilot plant using ilmenite as oxygen carrier, *Appl. Energy* 157 (2014) 288-294.
- [15] R. Pérez-Vega, A. Abad, F. García-Labiano, P. Gayán, L. F. de Diego and J. Adánez, Coal combustion in a 50 kWth Chemical Looping Combustion unit: Seeking operating conditions to maximize CO₂ capture and combustion efficiency, *Int. J. Greenh. Gas Control* 50 (2016) 80-92.
- [16] T. Mendiara, A. Abad, L. F. de Diego, F. García-Labiano, P. Gayán, and J. Adánez, Use of an Fe-Based Residue from Alumina Production as an Oxygen

Carrier in Chemical-Looping Combustion, *Energy Fuels* 26 (2012) 1420–1431.

[17] T. Mendiara, L. F. de Diego, F. García-Labiano, P. Gayán, A. Abad and J. Adánez, Behaviour of a bauxite waste material as oxygen carrier in a 500 Wth CLC unit with coal, *Int. J. Greenh. Gas Control* 17 (2013) 170-182

[18] M. Schmitz, C. Linderholm, P. Hallberg, S. Sundqvist and A. Lyngfelt, Chemical-Looping Combustion of Solid Fuels Using Manganese Ores as Oxygen Carriers, *Energy Fuels* 30 (2016) 1204-1216.

[19] P. Gayán, A. Abad, L. F. de Diego, F. García-Labiano and J. Adánez, Assessment of technological solutions for improving chemical looping combustion of solid fuels with CO₂ capture, *Chem. Eng. J.* 233 (2013) 56-69.

[20] T. Mattisson, A. Lyngfelt and H. Leion, Chemical-looping with oxygen uncoupling for combustion of solid fuels, *Int. J. Greenh. Gas Control*, 2009, 3, 11-19.

[21] A. Abad, I. Adánez-Rubio, P. Gayán, F. García-Labiano, L. F. de Diego and J. Adánez, Demonstration of chemical-looping with oxygen uncoupling (CLOU) process in a 1.5 kWth continuously operating unit using a Cu-based oxygen-carrier, *Int. J. Greenh. Gas Control* 6 (2012) 189-200.

[22] R. Pérez-Vega, A. Abad, J. Adánez, L.F. de Diego, F. García-Labiano and P. Gayán, Development of a Mn Development of a Mn -Fe -Ti based Oxygen Carrier in Chemical Looping Combustion with Coal, 7th International Conference of Clean Coal Technologies, Krakow, 17-21 May, 2015.

[23] J. Chiu, H. Andrus, Alstom's Chemical Looping Prototypes, Program Update, CO₂ Capture Technology Meeting, Pittsburg, PA, August, 2014.

- [24] I. Abdulally, C. Beal, A. Herbert, B. Epple, A. Lyngfelt and L. Bruce, Alstom's Chemical Looping Prototypes, Program Update, 37th Int. Technical Conf. 11 on Clean Coal & Fuel Systems, Clearwater, FL, USA, June, 2012.
- [25] A. Levasseur. Alstom's Limestone-based Chemical Looping Development For Advanced Gasification, DOE Workshop: Gasification Systems and Coal & Biomass to Liquids, Morgantown, WV, August, 2015.
- [26] Q. Song, R. Xiao, Z. Deng, L. Shen, J. Xiao and M. Zhang, Effect of Temperature on Reduction of CaSO₄ Oxygen Carrier in Chemical-Looping Combustion of Simulated Coal Gas in a Fluidized Bed Reactor, *Ind. Eng. Chem. Res.* 47 (2008) 8148-8159
- [27] Q. Song, R. Xiao, Z. Deng, W. Zheng, L. Shen and J. Xiao, Multicycle Study on Chemical-Looping Combustion of Simulated Coal Gas with a CaSO₄ Oxygen Carrier in a Fluidized Bed Reactor, *Energy Fuels*, 2008, 22, 3661-3672.
- [28] H. Tian, X. Hu, J. Chang, M. Han, G. Sun and Q. Guo, Simulation of a new chemical-looping combustion process without sulfur evolution based on ca-based oxygen carrier, *Int. J. Chem. React. Eng.* 12 (2014) 1-12.
- [29] Q. Song, R. Xiao, Z. Deng, H. Zhang, L. Shen, J. Xiao and M. Zhang, Chemical-looping combustion of methane with CaSO₄ oxygen carrier in a fixed bed reactor, *Energ. Convers. Manage.* 49 (2008) 3178-3187.
- [30] L. Shen, M. Zheng, J. Xiao and R. Xiao, A mechanistic investigation of a calcium-based oxygen carrier for chemical looping combustion, *Comb. Flame* 154 (2008) 489-506.
- [31] S. Zhang, R. Xiao, J. Liu and S. Bhattacharya, Performance of Fe₂O₃/CaSO₄ composite oxygen carrier on inhibition of sulfur release in calcium-based chemical looping combustion, *Int. J. Greenh. Gas Control* 17 (2013) 1-12.

- [32] T. Song, M. Zheng, L. Shen, T. Zhang, X. Niu and J. Xiao, Mechanism Investigation of Enhancing Reaction Performance with $\text{CaSO}_4/\text{Fe}_2\text{O}_3$ Oxygen Carrier in Chemical-Looping Combustion of Coal, *Int. Eng. Chem. Res.* 52 (2013) 4059-4071.
- [33] N. Ding, C. Zhang, C. Luo, Y. Zheng and Z. Liu, Effect of hematite addition to CaSO_4 oxygen carrier in chemical looping combustion of coal char, *RSC adv* 5 (2015) 56362-56376.
- [34] M. Zheng, L. Shen and X. Feng, In situ gasification chemical looping combustion of a coal using the binary oxygen carrier natural anhydrite ore and natural iron ore, *Energ. Convers. Manage.* 83 (2014) 270-283.
- [35] H. Tian, Q. Guo, X. Yue and Y. Liu, Investigation into sulfur release in reductive decomposition of calcium sulfate oxygen carrier by hydrogen and carbon monoxide, *Fuel Process. Technol.* 91 (2010) 1640-1649.
- [36] R. Xio and Q. Song, Characterization and kinetics of reduction of CaSO_4 with carbon monoxide for chemical-looping combustion, *Combust. Flame* 158 (2011) 2524-2539.
- [37] M. Zheng , L. Shen, X. Feng and J. Xiao, Kinetic Model for Parallel Reactions of CaSO_4 with CO in Chemical-Looping Combustion, *Ind. Eng. Chem. Res.* 50 (2011) 5414-5427.
- [38] H. Tian and Q. Guo, Investigation into the Behavior of Reductive Decomposition of Calcium Sulfate by Carbon Monoxide in Chemical-Looping Combustion, *Ind. Eng. Chem. Res.* 48 (2009) 5624-5632.
- [39] H. Tian, Q. Guo and J. Chang, Investigation into Decomposition Behavior of CaSO_4 in Chemical-Looping Combustion, *Energy Fuels*, 2008, 22, 3915-3921.

- [40] Y. Liu, Q. Guo, Y. Cheng and H-J Ryu, Reaction Mechanism of Coal Chemical Looping Process for Syngas Production with CaSO₄ Oxygen Carrier in the CO₂ Atmosphere, *Ind. Eng. Chem. Res.* 51 (2012) 10364-10373.
- [41] S. Zhang, R. Xiao, Y. Yang and L. Chen, CO₂ Capture and Desulfurization in Chemical Looping Combustion of Coal with a CaSO₄ Oxygen Carrier, *Chem. Eng. Technol.* 36 (2013) 1469-1478.
- [42] M. Zheng and L. Shen, In Situ Gasification Chemical Looping Combustion of Coal Using the Mixed Oxygen Carrier of Natural Anhydrite Ore and Calcined Limestone, *Int. J. Chem. Reactor Eng.* 14 (2016) 637-652.
- [43] E. J. Anthony and D. L. Granatstein, Sulfation phenomena in fluidized bed combustion systems, *Prog. Energ. Combust. Sci.* 27 (2001) 215–36.
- [44] J. H. Chiu, H. E. Andrus, G. N. Liljedahl, P. R. Thibeault. System for hot solids combustion and gasification. Patent WO 2010/014938 A9.
- [45] HSC Chemistry 6.1. Chemical Reaction and Equilibrium Software with Thermochemical Database and Simulation Module. Outotec Research Oy, Pori, Finland, 2008.
- [46] T. Mendiara, L. F. de Diego, F. García-Labiano, P. Gayán, A. Abad and J. Adánez, On the use of a highly reactive iron ore in Chemical Looping Combustion of different coals, *Fuel* 126 (2014) 239-249.
- [47] I. Barin, Thermochemical Data of Pure Substances. VCH, Weinheim, Germany, 1989.

- [48] A. Abad, J. Adánez, F. García-Labiano, L. F. de Diego, P. Gayán and J. Celaya, Mapping of the range of operational conditions for Cu-, Fe-, and Ni-based oxygen carriers in chemical-looping combustion, *Chem. Eng. Sci.* 62 (2007) 533-549.
- [49] M. de las Obras-Ioscertales, L. F. de Diego, F. García-Labiano, A. Abad, P. Gayán and J. Adánez, Sulfur retention in an oxy-fuel bubbling fluidized bed combustor: Effect of coal rank, type of sorbent and O₂/CO₂ ratio, *Fuel* 137 (2014) 384-392.
- [50] A. Cuadrat, A. Abad, F. García-Labiano, P. Gayán, L. F. de Diego and J. Adánez, Effect of operating conditions in Chemical-Looping Combustion of coal in a 500 Wth unit, *Int. J. Greenhouse Gas Control* 6 (2012) 153–163.
- [51] A. Abad, J. Adánez, P. Gayán, L. F. de Diego, F. García-Labiano and G. Sprachmann, Conceptual design of a 100 MWth CLC unit for solid fuel combustion, *Appl. Energ.* 157 (2015) 462-474.
- [52] Q. Guo, J. Zhang and H. Tian, Recent advances in CaSO₄ oxygen carrier for chemical-looping combustion (CLC) process, *Chem. Eng. Commun.* 199 (2012) 1463-1491.
- [53] A. Abad, J. Adánez, A. Cuadrat, F. García-Labiano, P. Gayán and L. F. de Diego, Kinetics of redox reactions of ilmenite for chemical-looping combustion, *Chem. Eng. Sci.* 66(2011) 689–702.
- [54] T. Mendiara, R. Pérez, A. Abad, L. F. de Diego, F. García-Labiano, P. Gayán, and J. Adánez, Low-Cost Fe-Based Oxygen Carrier Materials for the iG-CLC Process with Coal. 1, *Ind. Eng. Chem. Res.* 51 (2012) 16216–16229.
- [55] N. Berguerand and A. Lyngfelt, Chemical-Looping Combustion of Petroleum Coke Using Ilmenite in a 10 kWth Unit-High-Temperature Operation, *Energy Fuels* 23 (2009) 5257-5268.

- [56] Q. Guo, X. Hu, Y. Liu, W. Jia, M. Yang, M. Wu, H. Tian and H. J. Ryu, Coal chemical-looping gasification of Ca-based oxygen carriers decorated by CaO, *Powder Technology* 275 (2015) 60-68.
- [57] F. García-Labiano, A. Rufas, L. F. de Diego, M. de las Obras-Loscertales, P. Gayán, A. Abad and J. Adánez, Calcium-based sorbents behaviour during sulphation at oxy-fuel fluidised bed combustion conditions, *Fuel* 90 (2011) 3100-3108.
- [58] F. García-Labiano, A. Abad, L. F. de Diego, P. Gayán, and J. Adánez, Calcination of calcium-based sorbents at pressure in a broad range of CO₂ concentrations, *Chem. Eng. Sci.* 57 (2002) 2381-2393.
- [59] J. Adánez, L. F. de Diego, F. García-Labiano and A. Abad, Kinetics of H₂S Reaction with Calcined Calcium-Based Sorbents, *Energy Fuels* 12 (1998) 617-625.
- [60] G. Marbán, M. García-Calzada, A. B. Fuertes, Kinetics of oxidation of CaS particles in the regime of low SO₂ release, *Chem. Eng. Sci.* 54 (1999) 77-90.

CAPTIONS FOR TABLES AND FIGURES

Table 1 Chemical reactions involved in iG-CLC using CaSO_4 as oxygen carrier.

Table 2 Proximate and ultimate analysis of the coals (wt.%).

Table 3 Data and equations used to calculate mass balances. Basis for calculation: \dot{m}_{coal} (kg/s) corresponding to a 1 MW_{th} .

Table 4 Chemical composition (wt.%) of Granicarb limestone.

Fig. 1 General scheme of iG-CLC process.

Fig. 2 Flow diagram of iG-CLC process using limestone as oxygen carrier precursor and sulphur sorbent.

Fig. 3 Thermodynamic equilibrium compounds in the fuel reactor as a function of A) temperature; B) oxygen carrier to fuel ratio (ϕ) for gas and solids phases. $[\text{S}/\text{C}] = 0.1$; $[\text{H}_2\text{O}/\text{C}] = 1$; $[\text{CaSO}_4/\text{CaO}] = 1$.

Fig. 4 Thermodynamic equilibrium compounds in the air reactor as a function of the temperature for gas and solid phases. $\text{CaSO}_4:\text{CaS}:\text{CaO} = 1: 1: 1$.

Fig. 5 Fate of CaSO_4 and CaS in the fuel reactor. Case I: $\text{SR} = 0\%$, $[\text{Ca}/\text{S}]$ molar ratio = 0 and $\phi = 1$. Case II: $\text{SR} = 100\%$, $[\text{Ca}/\text{S}]$ molar ratio = 1 and $\phi = 1$.

Fig. 6 Composition of the recirculated stream from air reactor as well as the corresponding oxygen transport capacity for the three coals selected. $\text{SR} = 100\%$, Any ϕ .

Fig. 7 Solids recirculation rate as a function of the oxygen carrier to fuel ratio at different [Ca/S] molar ratio for the three coals selected.

Fig. 8 Effect of oxygen carrier to fuel ratio on the air reactor temperature at different [Ca/S] molar ratio for the three coals selected.

Fig. 9 Influence of the oxygen carrier-to-fuel ratio (ϕ) molar ratio on the heat extracted from air reactor at different [Ca/S] molar ratio for the three coals selected.

Fig. 10 Comparison of the Influence of oxygen carrier to fuel ratio and [Ca/S] molar ratio on solids circulation rate, temperature and heat extracted from air reactor for SR=100% and SR= 54%. Coal: Teruel lignite. [Ca/S] = 3. TFR= 950 °C.

Fig. 11 Effect of ash and sulfur content of coal on: A) solids circulation rate; B) oxygen transport capacity; C) air reactor temperature; D) heat extracted from air reactor. Oxygen carrier to fuel ratio $\phi = 10$; [Ca/S] =3.

Fig. 12 Initial redox cycles obtained in TGA with the Granicarb limestone

Fig. 13 Redox cycles of sulfated limestone alternating H₂ and air in TGA, including limestone sulfidation with H₂S during reduction period.

Fig. 14. Fraction of CaSO₄ and the [S/Ca] molar ratio as a function of the number of redox cycles.

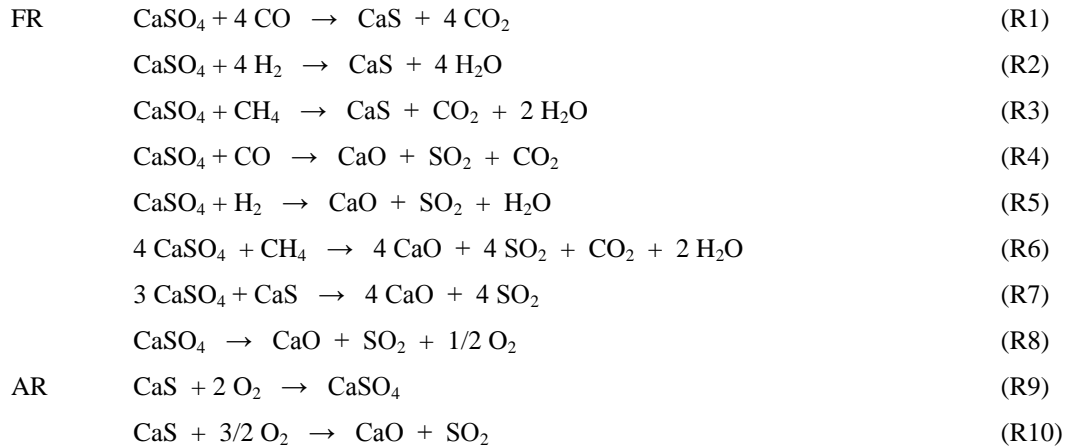
Fig. 15 Comparison of the evolution with the number of redox cycles between the effective and theoretical oxygen transport capacity.

Fig. 16 Influence of the Ca/S molar ratio on the solids circulation at different values of sulphur retention for the three coals used. Red line: expected sulphur retention for Granicarb limestone.

Submitted, accepted and published by:
Chemical Engineering Journal 310 (2017) 226-239

Table 1 Chemical reactions involved in iG-CLC using CaSO₄ as oxygen carrier.

CLC related chemical reactions



Reactions involving limestone and sulphur in coal

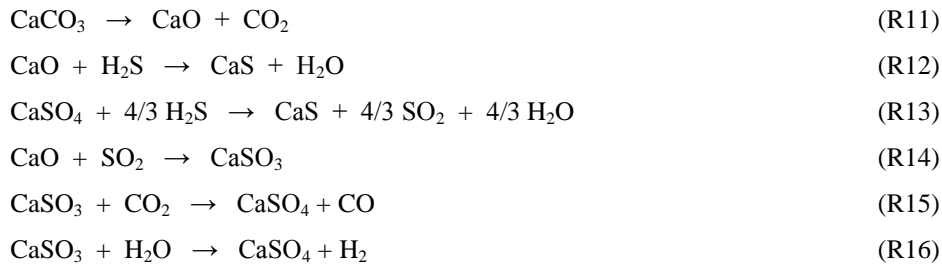


Table 2 Proximate and ultimate analysis of the coals (wt.%).

Coal	Sub-bituminous	Lignite	Lignite
	Chilean	Teruel	Alcorisa
Moisture	14.3	12.6	11.1
Ash	15.3	25.2	11.3
Volatiles	34.6	28.7	38.6
Fixed carbon	35.8	33.6	39.0
C	52.4	45.4	54.7
H	3.6	2.5	4.1
N	0.8	0.6	0.4
S	0.2	5.2	8.1
O*	13.4	8.5	10.3
LHV (kJ/kg)	18910	16251	20837
Ω_{coal} (mol O/kg coal)	97	86	110

Table 3 Data and equations used to calculate mass balances. Basis for calculation: \dot{m}_{coal} (kg/s) corresponding to a 1 MW_{th}.

Fuel reactor	
$F_{in,FR}$	$F_{out,FR}$
$coal = n_C + n_H + n_S + n_N + n_O + n_{ash} + n_{H_2O,moist}$ $n_{H_2O,gasif} = n_C [H_2O / C]$ $n_{CaCO_3,inFR} = n_S [Ca / S]$ $n_{CaSO_4,AR \rightarrow FR} = \frac{\phi \Omega_{coal} \dot{m}_{coal}}{4}$ $n_{CaO,AR \rightarrow FR} = \left([Ca / S] \frac{1}{SR} - 1 \right) n_{CaSO_4,AR \rightarrow FR}$ $n_{ash,AR \rightarrow FR} = \left(n_{CaSO_4,AR \rightarrow FR} + n_{CaO,AR \rightarrow FR} \right) \frac{n_{ash}}{n_{CaCO_3}}$	$n_{N_2} = \frac{n_N}{2} ; n_{H_2} = \frac{n_H}{2} (1 - \eta_{comb}) ; n_{CO} = n_C (1 - \eta_{comb})$ $n_{SO_2} = n_S (1 - SR)$ $n_{CO_2,outFR} = n_C \eta_{comb} + n_{CO_2,CaCO_3inFR}$ $n_{H_2O,outFR} = \frac{n_H}{2} \eta_{comb} + n_{H_2O,moist} + n_{H_2O,gasif}$ $n_{ash,outFR} = n_{ash} + n_{ash,AR \rightarrow FR}$ $n_{CaS,SR} = n_S SR$ $n_{CaO,remain} = n_{CaCO_3,inFR} - n_{CaS,SR}$ $n_{CaO,outFR} = n_{CaO,remain} + n_{CaO,AR \rightarrow FR}$ $n_{CaS,red} = n_{CaSO_4,AR \rightarrow FR} \Delta X_s - \frac{n_{CaS,SR}}{4} - \frac{n_{CaS,SR}}{2}$ $n_{CaS,outFR} = n_{CaS,SR} + n_{CaS,red}$ $n_{CaSO_4,outFR} = n_{CaSO_4,AR \rightarrow FR} (1 - \Delta X_s) + \frac{n_{CaS,SR}}{4} + \frac{n_{CaS,SR}}{2}$
Air reactor	
$F_{in,AR} = F_{out,FR}$	$F_{AR \rightarrow FR} = F_{out,AR} - F_{PURGE}$
$F_{out,AR}$	F_{PURGE}
$n_{ash,outAR} = n_{ash,outFR}$ $n_{CaO,outAR} = n_{CaO,outFR}$ $n_{CaO,inAR} = n_{CaO,outFR}$ $n_{CaSO_4,outAR} = n_{CaS,outFR} + n_{CaSO_4,outFR}$	$n_{ash,purge} = n_{ash}$ $n_{CaO,purge} = n_{CaO,outAR} \frac{n_{ash,purge}}{n_{ash,outAR}}$ $n_{CaSO_4,purge} = n_{CaSO_4,outAR} \frac{n_{ash,purge}}{n_{ash,outAR}}$

Table 4 Chemical composition (wt.%) of Granicarb limestone.

CaCO ₃	97.1
MgCO ₃	0.2
Na ₂ O	1.1
SiO ₂	<0.1
Al ₂ O ₃	<0.1
Fe ₂ O ₃	<0.1

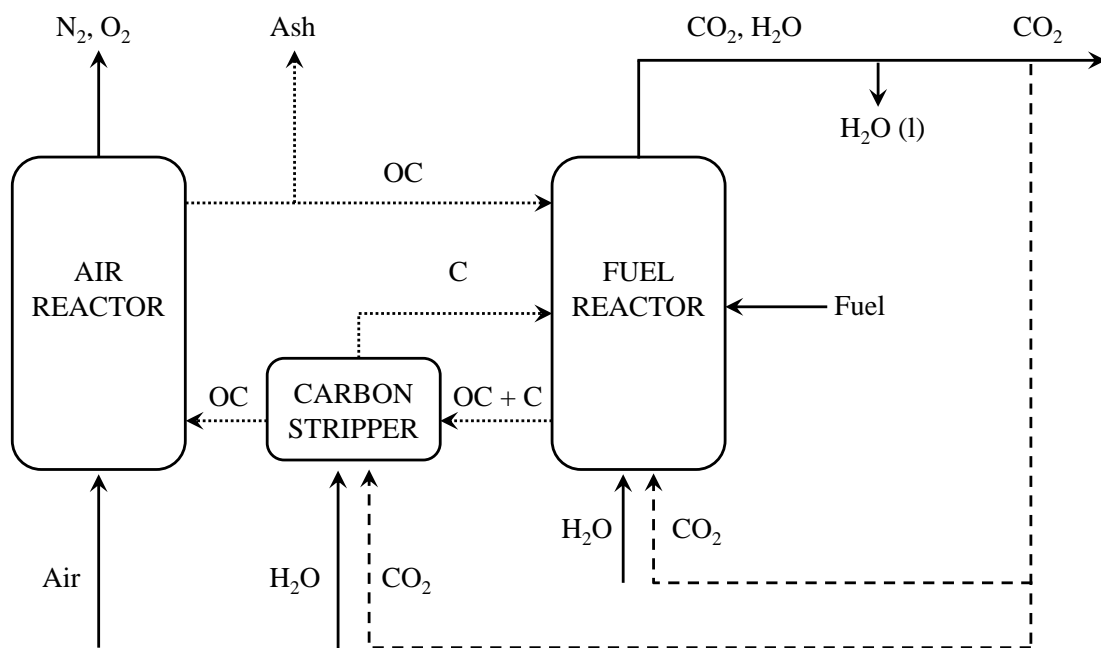


Fig. 1 General scheme of *i*G-CLC process.

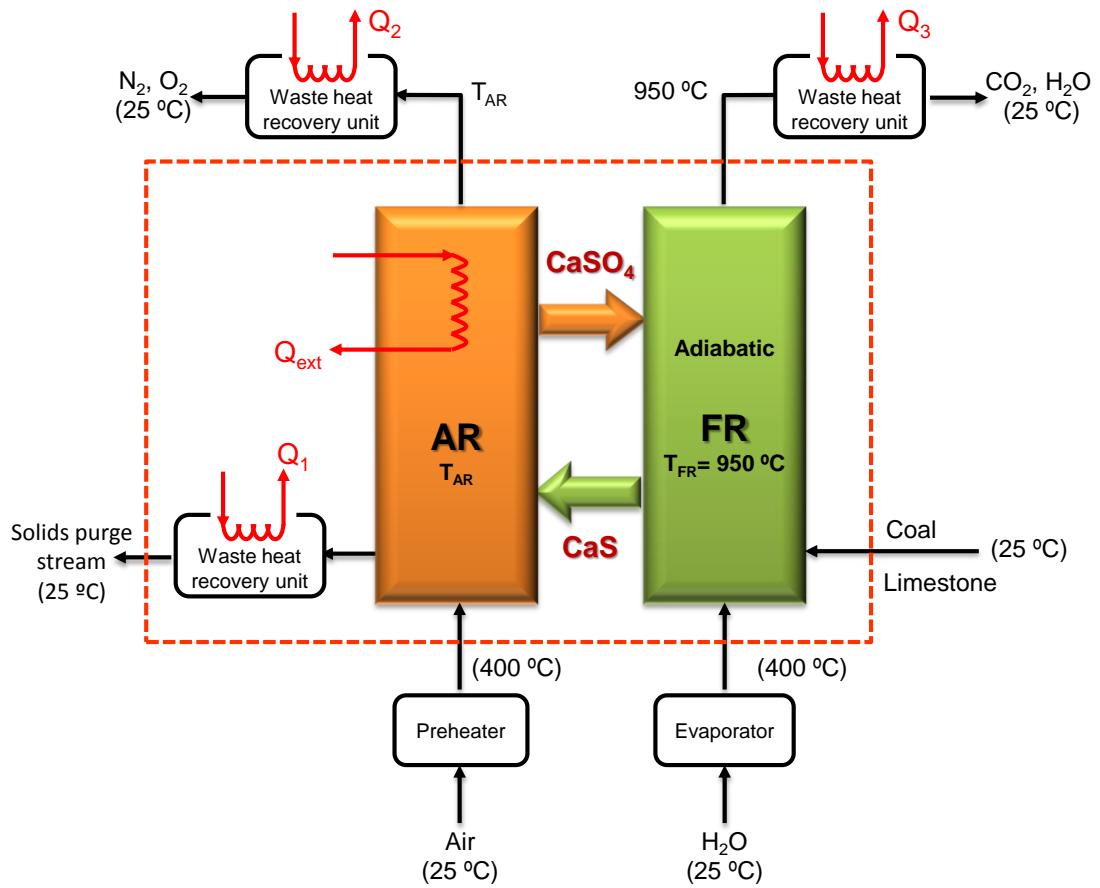


Fig. 2 Flow diagram of iG-CLC process using limestone as oxygen carrier precursor and sulphur sorbent.

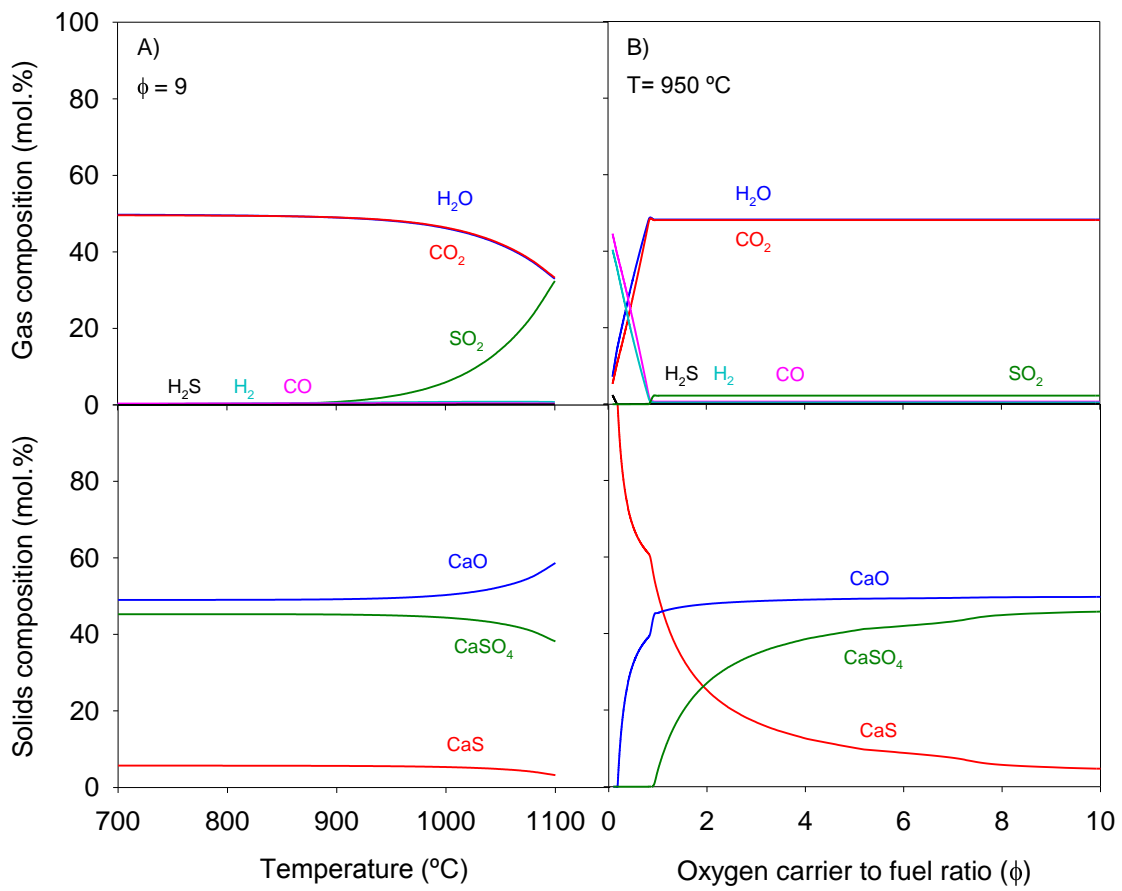


Fig. 3 Thermodynamic equilibrium compounds in the fuel reactor as a function of A) temperature; B) oxygen carrier to fuel ratio (ϕ) for gas and solids phases. $[\text{S}/\text{C}] = 0.1$; $[\text{H}_2\text{O}/\text{C}] = 1$; $[\text{CaSO}_4/\text{CaO}] = 1$.

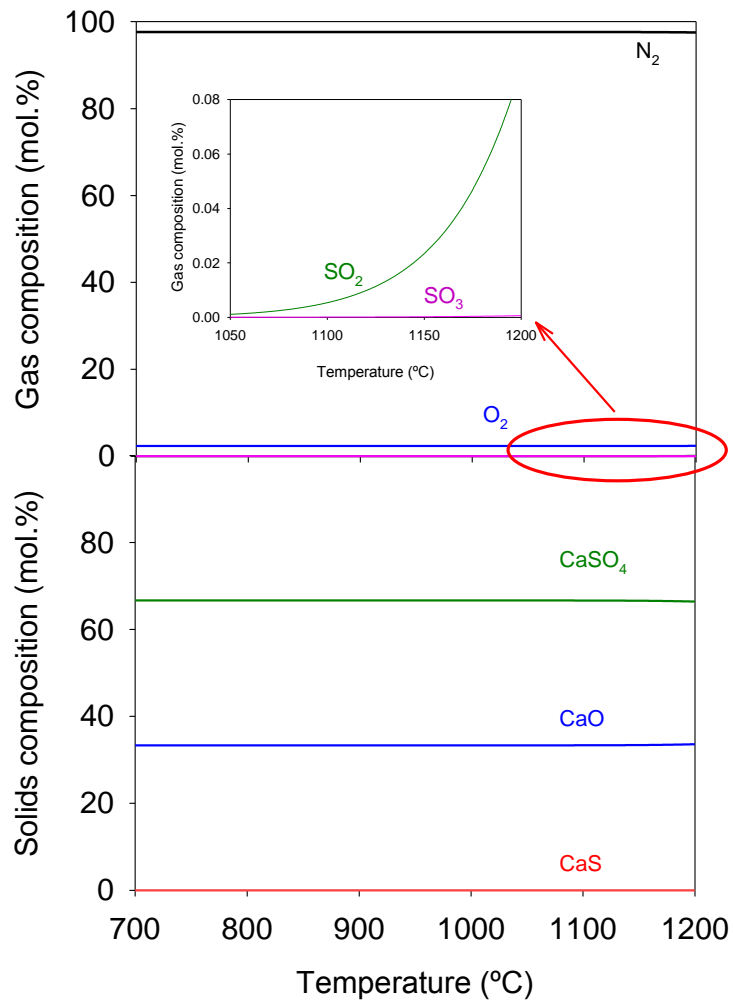


Fig. 4 Thermodynamic equilibrium compounds in the air reactor as a function of the temperature for gas and solid phases. CaSO₄:CaS:CaO= 1: 1: 1.

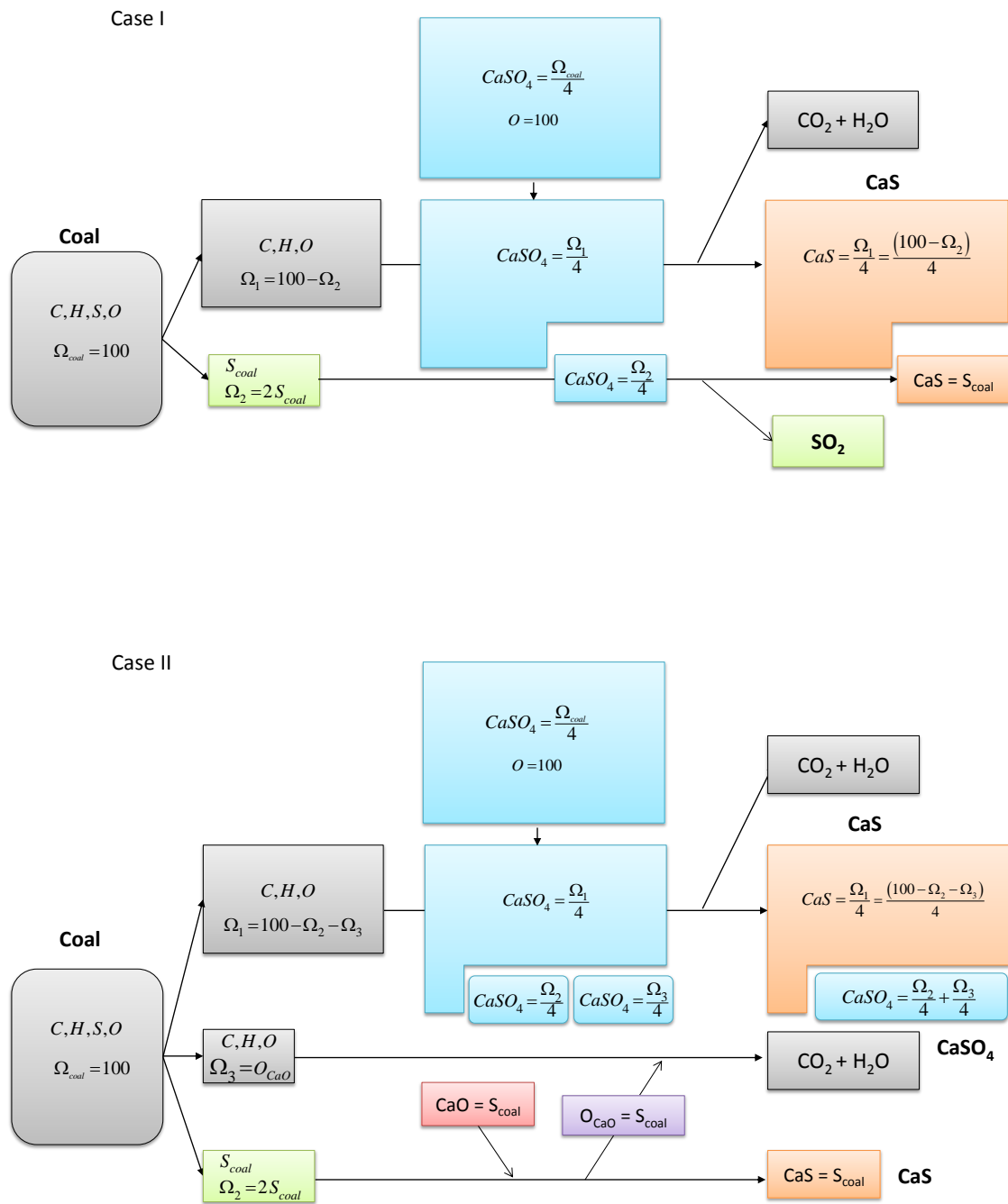


Fig. 5 Fate of $CaSO_4$ and CaS in the fuel reactor. Case I: SR = 0 %, [Ca/S] molar ratio = 0 and $\phi = 1$.
 Case II: SR = 100 %, [Ca/S] molar ratio = 1 and $\phi = 1$.

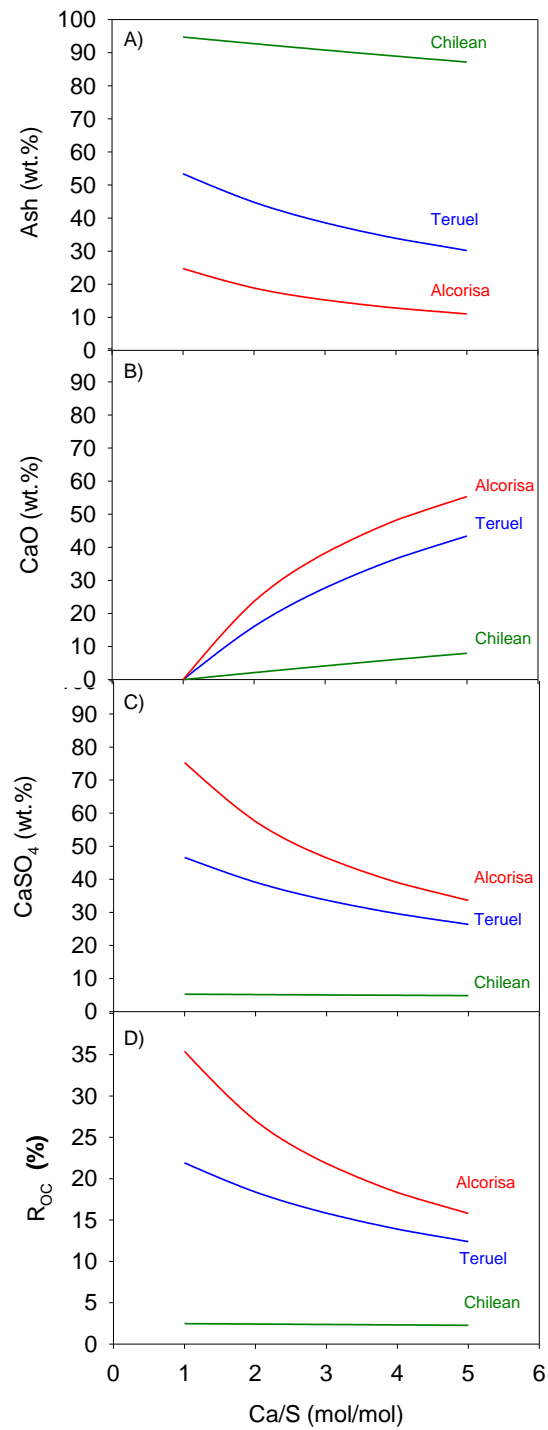


Fig. 6 Composition of the recirculated stream from air reactor as well as the corresponding oxygen transport capacity for the three coals selected. SR=100 %, Any ϕ .

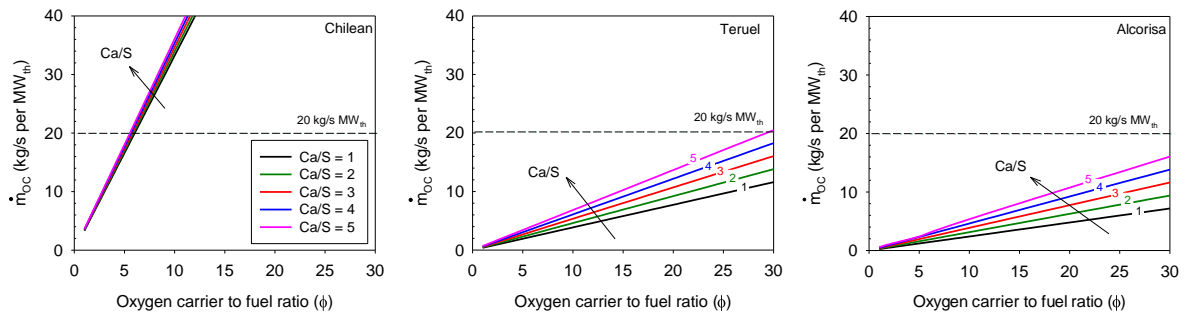


Fig. 7 Solids recirculation rate as a function of the oxygen carrier to fuel ratio at different [Ca/S] molar ratio for the three coals selected.

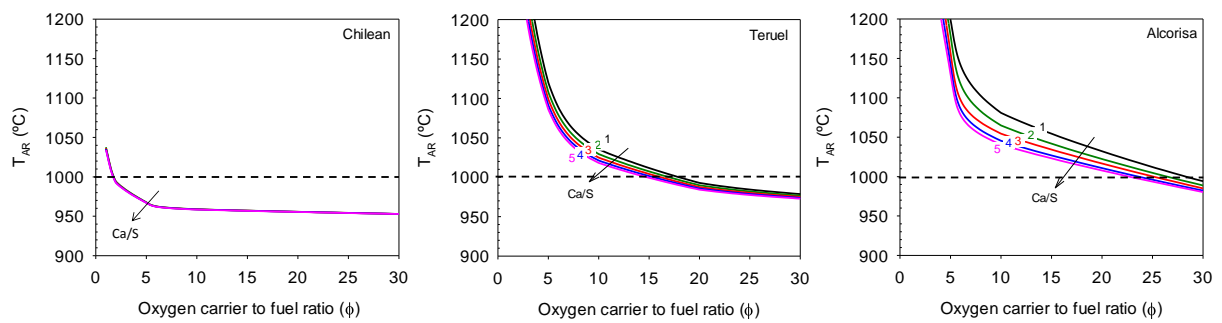


Fig. 8 Effect of oxygen carrier to fuel ratio on the air reactor temperature at different [Ca/S] molar ratio for the three coals selected.

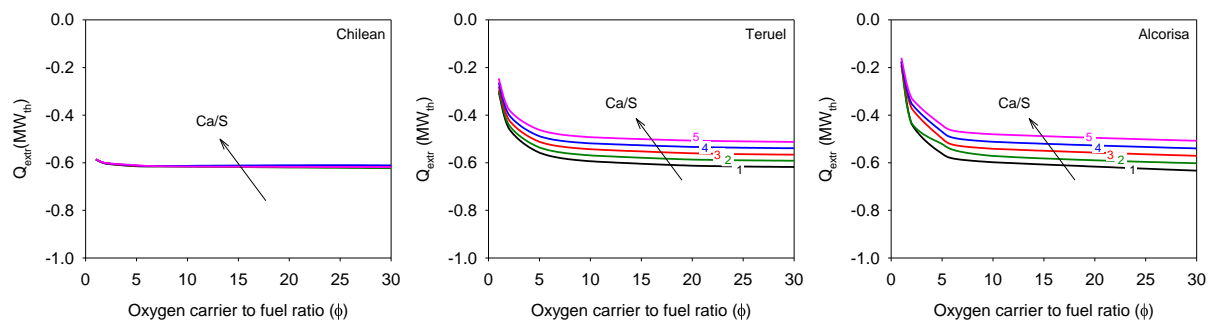


Fig. 9 Influence of the oxygen carrier-to-fuel ratio (ϕ) molar ratio on the heat extracted from air reactor at different [Ca/S] molar ratio for the three coals selected.

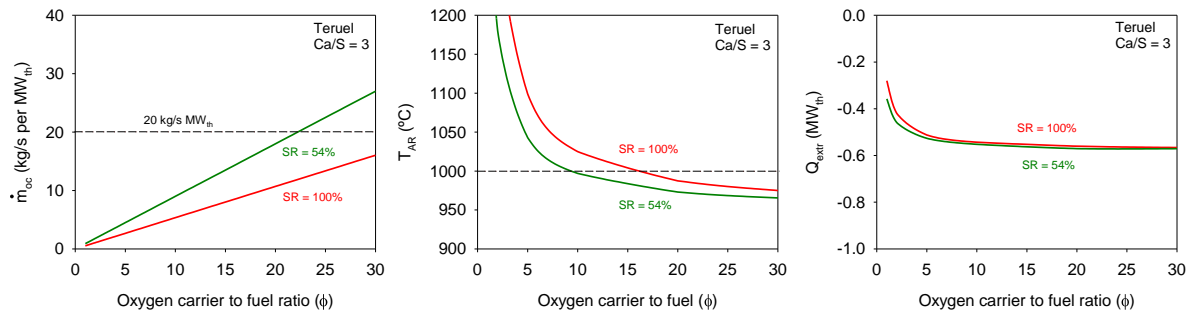


Fig. 10 Comparison of the Influence of oxygen carrier to fuel ratio and [Ca/S] molar ratio on solids circulation rate, temperature and heat extracted from air reactor for SR=100% and SR= 54%. Coal: Teruel lignite. [Ca/S] = 3. T_{FR} = 950 °C.

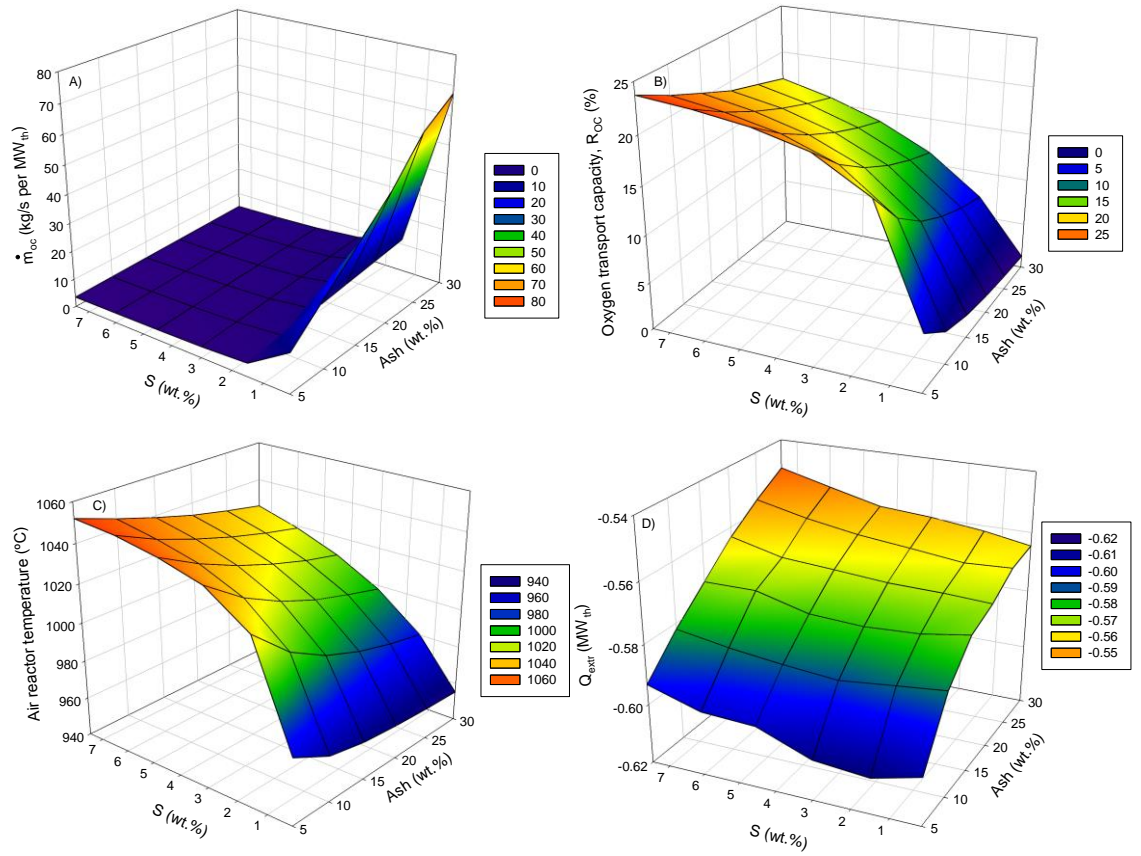


Fig. 11 Effect of ash and sulphur content of coal on: A) solids circulation rate; B) oxygen transport capacity; C) air reactor temperature; D) heat extracted from air reactor. Oxygen carrier to fuel ratio $\phi = 10$; $[Ca/S] = 3$.

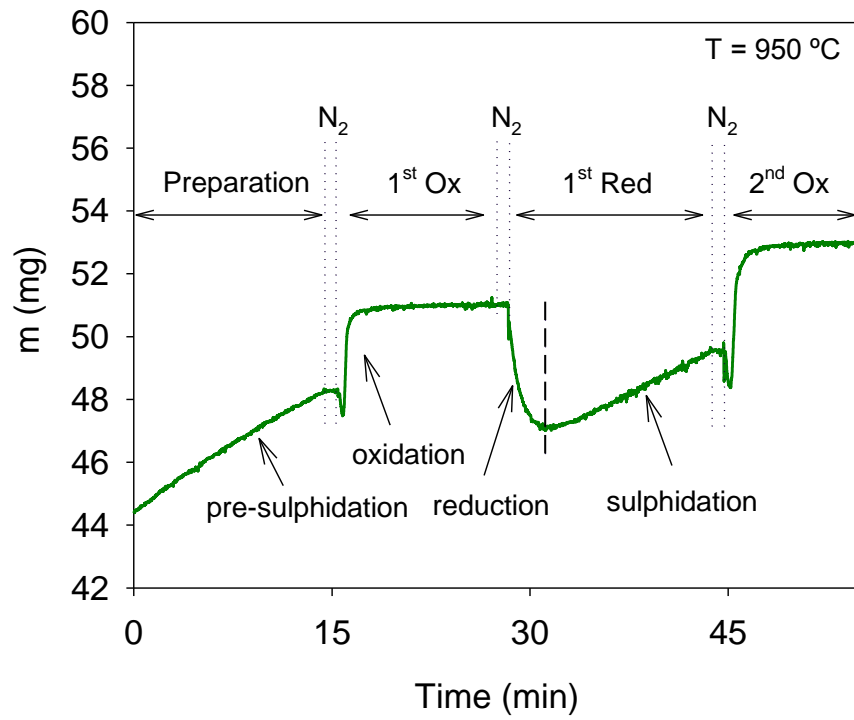


Fig. 12 Initial redox cycles obtained in TGA with the Granicarb limestone.

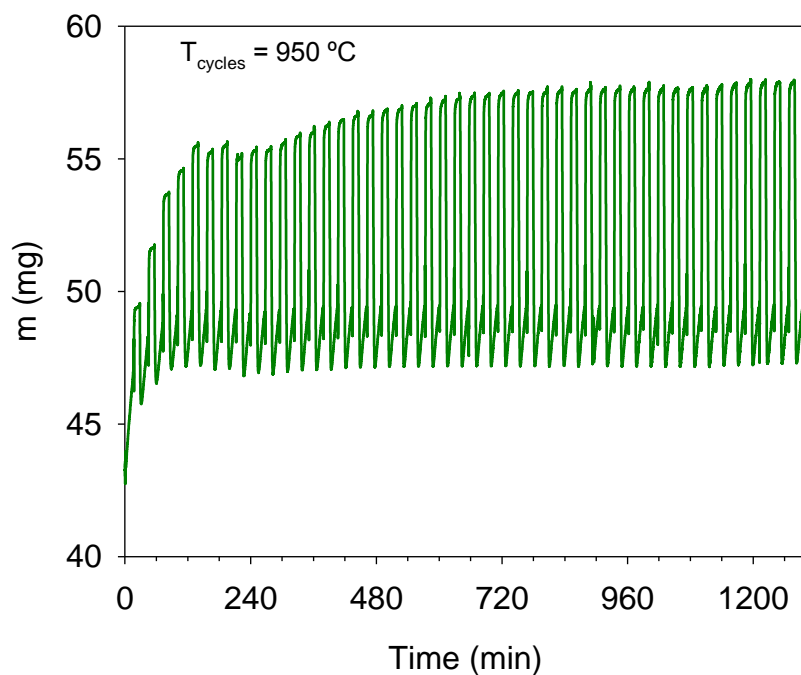


Fig. 13 Redox cycles of sulphated limestone alternating H_2 and air in TGA, including limestone sulphidation with H_2S during reduction period.

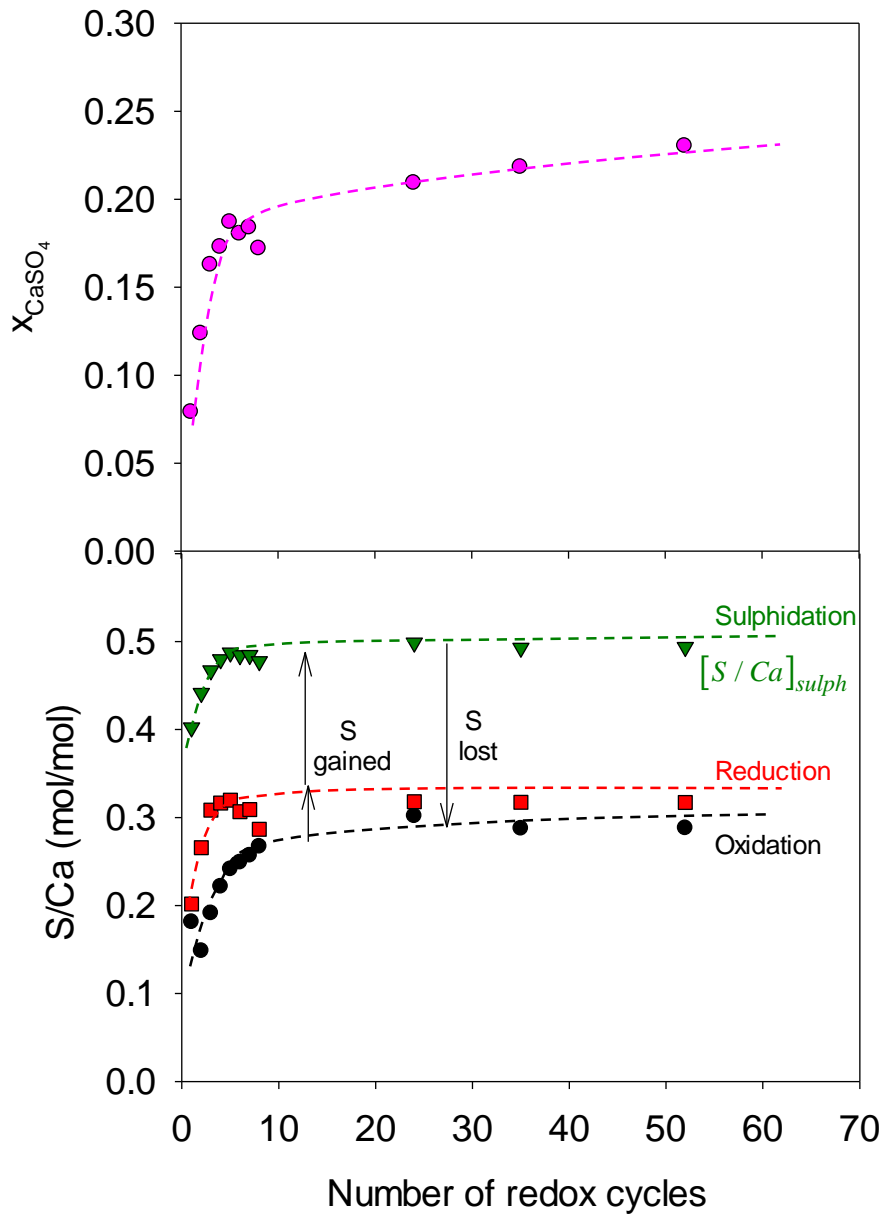


Fig. 14 Fraction of CaSO_4 and the $[\text{S}/\text{Ca}]$ molar ratio as a function of the number of redox cycles.

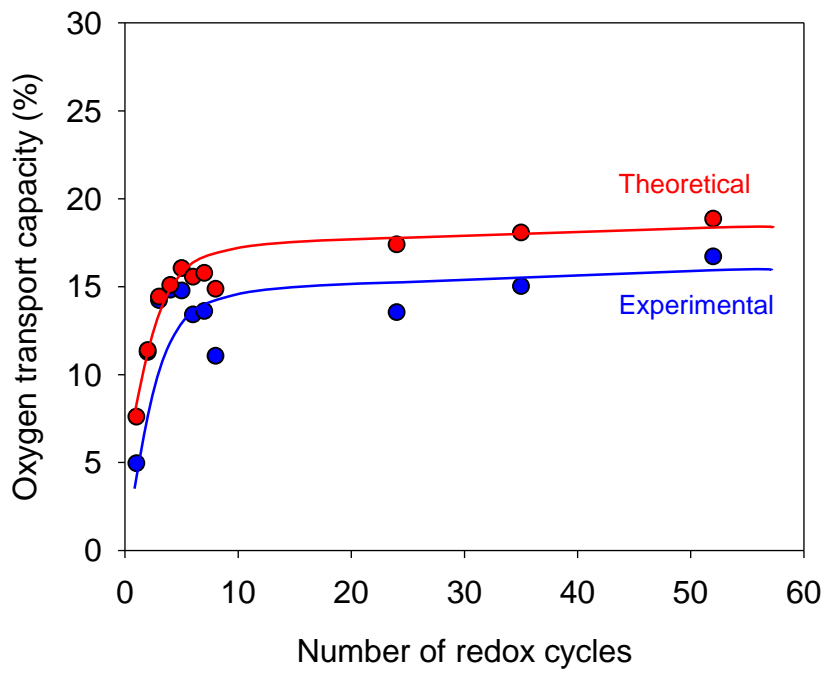


Fig. 15 Comparison of the evolution with the number of redox cycles between the effective and theoretical oxygen transport capacity.

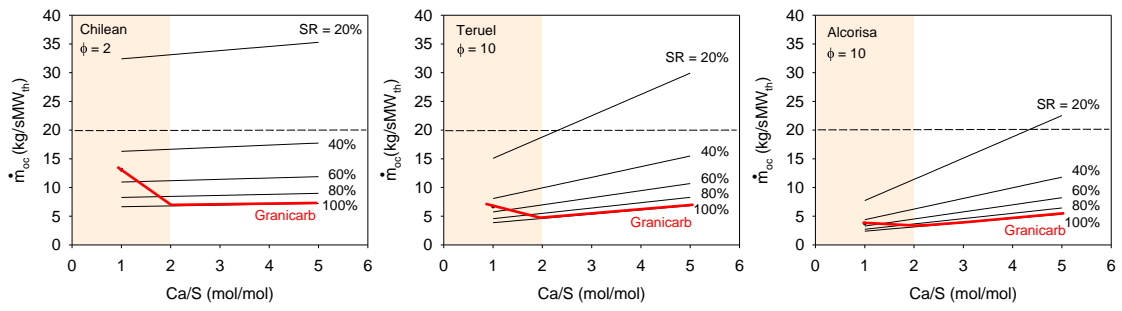


Fig. 16 Influence of the Ca/S molar ratio on the solids circulation at different values of sulphur retention for the three coals used. Red line: expected sulphur retention for Granicarb limestone.